



**Codes And Methods Improvements  
for VVER comprehensive safety assessment**

Grant Agreement Number: 945081

Start date: 01/09/2020 - Duration: 36 Months

---

**WP5 - Task 5.2**

**D5.3 - Results of neutronics and closed channel  
thermal-hydraulics coupling small core  
calculations**

---

B. Vezzoni, B. Calgaro (Framatome)  
F. Damian (CEA)  
G. Huaccho Zavala (KIT)

Version 1 – 31/08/2023



This project has received funding from the Euratom research and training programme 2019-2020 under grant agreement No 945081

Document title	Results of neutronics and closed channel thermal-hydraulics coupling small core calculations
Author(s)	B. Vezzoni, B. Calgaro, F. Damian, G. Huaccho Zavala
Document type	Deliverable
Work Package	WP5
Document number	D5.3 – version 1
Issued by	CEA
Date of completion	31/08/2023
Dissemination level	Public

### Summary




The present document corresponds to Deliverable 5.3 “Results of neutronics and closed channel thermal-hydraulics coupling small core calculations” of the CAMIVVER project. This document presents modeling and first results obtained on VVER small core configuration based on CEA code APOLLO3®. As first step of the study, VVER APOLLO3® core model was defined using neutronic data libraries already available before moving to successive versions of MPOs generated by the embedded APOLLO3® in NEMESI lattice solver provided from WP4.

The Deliverable 5.3 describes initially the small core VVER 7 FAs test case identified at the beginning of the project. This configuration is adapted for sensitivity analysis, improvement of participants competencies in benchmark definition and first comparisons on VVER hexagonal geometries.

This simplified model will allow providing further elements for the verification of the neutronics data libraries, MPOs, generated in WP4 and first elements to analyze the TH feedbacks for a typical VVER geometry for tests cases defined in Task 5.1.

For the transients selected at Task 5.1, benchmark comparisons against independent codes such as SERPENT2/SUBCHANFLOW (KIT) are proposed too. In order to provide a first attempt and comparison with a high-fidelity solution, large attention has been dedicated to core modeling, MPOs tests and feedbacks to WP4, steady-state calculations. In a second step during the very last months, the final version of neutron data libraries generated by the NEMESI have been adopted and used for final verification of the data to ensure expected progress with APOLLO3® at lattice and core level for steady-state and transient and its first usage in R&D activities by industrial partners.

### Approval

Version	First Author	WP leader	Project Coordinator
1	F. Damian (CEA) 31/08/2023	L. Mercatali (KIT) 31/08/2023	D. Verrier (Framatome) 31/08/2023
	Signature 1 <sup>st</sup> author 	Signature WP leader 	Signature Coordinator 

## Table of contents

1.	Introduction.....	10
2.	Context of VVER advanced core calculations.....	11
3.	WP5 task 5.2 main objectives .....	12
3.1.	Core description .....	12
3.2.	Core description .....	15
4.	Transient Scenario .....	18
4.1.1.	Initial conditions.....	18
4.1.2.	Transient conditions .....	19
4.2.	Output Parameters .....	19
5.	Summary of major results for the 7 FAs VVER test case.....	21
5.1.	APOLLO3®/THEDI code description .....	21
5.2.	7 FAs VVER core test case.....	22
5.3.	The high-fidelity solutions (KIT).....	23
5.3.1.	<i>The APOLLO3®-based solutions</i> .....	26
5.4.	Results and discussions.....	27
5.4.1.	Core reactivity characterization and first steady-state results.....	27
5.4.2.	Preliminary analyses of mid-term point comparisons.....	27
5.4.3.	Last discussions and improvements .....	30
6.	Conclusions.....	36
6.1.	Perspectives.....	36
	Appendix A : APOLLO3 CR worth sensitivity analysis.....	37
	Appendix B: SERPENT2/SCF sensitivity analysis and additional results.....	38

## List of Figures

Figure 1 Hexagonal Unit Cell (based on [5]) .....	13
Figure 2 Fuel Pin Cell (based on [5]) .....	13
Figure 3 Guide Tube with Absorber (based on [5]) .....	14
Figure 4 Central Tube Cell (based on [5]).....	14
Figure 5: 30AV5 without (left) and with (right) Control Rods (CRs) (based on [5]) .....	15
Figure 6 : Fuel Assembly 390GO without Control Rods (CRs based on [5]) .....	15
Figure 7: VVER Minicore Layout (based on [5]) .....	16
Figure 8: VVER minicore radial, top and bottom reflectors (based on [5]).....	17
Figure 9: Initial steady-state definition approach .....	18
Figure 10: 7 FAs VVER mini-core.....	21
Figure 11: APOLLO3® solver available. ....	22
Figure 12. SUBCHANFLOW fuel-centered model at pin/subchannel level. ....	24
Figure 13. radial and axial SERPENT2 model details. ....	25
Figure 14. fuel ifc file's header .....	25
Figure 15. coolant ifc file's header. ....	25
Figure 16: VVER mini-core: SERPENT2/SCF axially integrated normalized pin radial power distribution for the state before the transient (a) and at peak time (b) [15] .....	28
Figure 17: VVER mini-core: SERPENT2/SCF center fuel temperature (left) and coolant temperature (right) distribution at $t=0.12$ s [15].....	29
Figure 18: VVER mini-core: reactivity and POWER evolution[15] .....	30
Figure 19: 7 FAs VVER mini-core: Last comparison reactivity transient with first and final results (a) and a zoom on final results (b). ....	34
Figure 20: 7 FAs VVER mini-core: Last comparison POWER transient with first and final results (a) and a zoom on final results (b). ....	35
Figure 21. (top) core reactivity evolution in time. (bottom) standard deviation associated to the monte carlo simulation. vertical line marks the time when control rod is totally extracted. ....	39
Figure 22. (top) normalized core power evolution in time. (bottom) standard deviation associated to the monte carlo simulation. vertical line marks the time when control rod is totally extracted. ....	40

Figure 23. (right) axially integrated normalized pin power before the transient in case c. (left) axially averaged 1 sigma standard deviation. ....	41
Figure 24. (right) axially integrated normalized pin power at peak time for case c. (left) axially averaged 1 sigma standard deviation. ....	41
Figure 25. maximum centerline fuel temperature evolution in time.....	42
Figure 26. maximum outer surface fuel temperature evolution in time. ....	42
Figure 27. rod axially averaged centerline fuel temperature before and at 0.682 seconds of the transient (case c). ....	43
Figure 28. maximum internal surface cladding temperature evolution in time. ....	43
Figure 29. maximum external surface cladding temperature evolution in time. ....	44
Figure 30. maximum coolant temperature evolution in time. ....	44
Figure 31. subchannel axially averaged coolant temperature before and at 0.682 seconds of the transient (case c). ....	45
Figure 32. minimum dnb ratio evolution in time with W-3. ....	45

## Acronyms

APEX	APollo EXchange file
API	Application Programming Interface
BOC	Begin Of Cycle (of a fuel assembly in a nuclear reactor)
BWR	Boiling Water Reactor
CAL_RS	CALculation back-end Requirements Specification
CEA	Commissariat à l'Énergie Atomique et aux énergies alternatives
CPU	Central Processing Unit
CZP	Cold Zero Power
DDM	Domain Decomposition Method
DOM	Discrete Ordinates Method
EDF	Électricité de France
EOC	End Of Cycle (of a fuel assembly in a nuclear reactor)
EPR	European Pressurised Reactor / Evolutionary Power Reactor
FEM	Finite Element Method
FHS	Filesystem Hierarchy Standard
FLOPS	Floating Point Operations per Second
FS	Fine Structure
GiB	Gibibyte - $2^{30}$ bytes
HDF	Hierarchical Data Format
HFP	Hot Full Power
HPC	High Performance Computing
HZP	Hot Zero Power
IC-CPM	Interface Current Collision Probability Method
ISO	International Organization for Standardization
JHR	Jules Horowitz Reactor
KAIST	Korean Advanced Institute for Science and Technology
LWR	Light Water Reactor
MDL_RS	Multi-parameter Data Library Requirements Specification
MOC	Method Of Characteristics
MPI	Message Passing Interface
MPO	Multi Parametric Output
PBS	Portable Batch System
PWR	Pressurized Water Reactor
QoI	Quantity of Interest
RAM	Random Access Memory
RFC	Request For Comments
RMS	Root Mean Square
SFR	Sodium-cooled Fast Reactor

SHEM	Santamarina Hfaiedh Energy Mesh
SMR	Small Modular Reactor
Sn	Segment n
SPH	“SuPer-Homogénéisation”
SPn	Simplified Pn (Spherical Harmonics)
SYS_RS	System Requirements Specification
UC	Use Cases specification
UDM	User Data Model
VVER	Vodo-Vodyanoi Energetichesky Reaktor (water-water power reactor)
WP	Work Package

## References

- [1] Codes and Methods Improvement for VVER Comprehensive Safety Assessment – H2020 CAMIVVER Project – Grant Agreement n. 945081.
- [2] J. Blanco and B. Calgaro, "Description of the core reference test cases - Part 1," CAMIVVER Deliverable 5.1, 2021.
- [3] G. Huaccho Zavala, B. Calgaro, B. Vezzoni, "Description of the core reference test cases – Part 1 + Part 2", CAMIVVER H2020 Deliverable 5.2, 2023
- [4] B. Calgaro, B. Vezzoni, G. Huaccho Zavala, "First step to a reference multi-physics approach: results of 3D neutronics and thermal-hydraulics coupling small core calculations", CAMIVVER H2020 Deliverable 5.4, 2023
- [5] WILLIEN, A. and VEZZONI, B. 11/02/2021. D4.3 – Definitions of tests cases for the verification phases of the multi-parametric library generator. Version 1. CAMIVVER. H2020.
- [6] Qualification of scientific computing tools used in the nuclear safety case – 1st barrier, <https://www.french-nuclear-safety.fr/asn-regulates/asn-guides/asn-guide-no.-28>
- [7] D4.1 - Representative use cases and specification requirements for the prototype multiparametric libraries generator. CAMIVVER. H2020.
- [8] B. Calgaro, B. Vezzoni, "The CAMIVVER EU Horizon 2020 project", presentation at OECD/NEA 22/02/2023.
- [9] P. Mosca, L. Bourhrara, A. Calloo, A. Gammicchia, F. Goubioud et al. (2023), "APOLLO3@: Overview of the new code capabilities for reactor physics analysis," Proceeding International Conference M&C2023, Niagara Falls, Ontario, Canada, August 13-17, 2023.
- [10] J. Leppänen, "The Serpent Monte Carlo code: Status development and applications in 2013," *Ann. Nucl. Energy*, 82, pp. 142-150, 2015.
- [11] U. Imke and V. Sanchez, "Validation of the Subchannel Code SUBCHANFLOW using the NUPEC PWR Tests (PSBT)," *Science and Technology of Nuclear Installations*, vol. 12, 2012.
- [12] D. Ferraro, M. García, V. Valtavirta, U. Imke, R. Tuominen, J. Leppänen and V. Sanchez-Espinoza, "Serpent/SUBCHANFLOW pin-by-pin coupled transient calculations for the SPERT-III hot full power tests," *Annals of Nuclear Energy*, vol. 142, 2020.
- [13] D. Ferraro, M. García, U. Imke, V. Valtavirta, R. Tuominen, Y. Bilodid, J. Leppänen and V. Sanchez-Espinoza, "SERPENT/SUBCHANFLOW COUPLED CALCULATIONS FOR A VVER CORE AT HOT FULL POWER," in *PHYSOR 2020*, Cambridge, United Kingdom, 2020.
- [14] D. Ferraro, M. García, V. Valtavirta, U. Imke, R. Tuominen, J. Leppänen and V. Sanchez-Espinoza, "Serpent/SUBCHANFLOW pin-by-pin coupled transient calculations for a PWR minicore," *Annals of Nuclear Energy*, vol. 137, 2020
- [15] L. Mercatali, G. Huaccho, B. Calgaro, B. Vezzoni, P. Mosca, V.H. Sanchez-Espinoza, "Advanced Multiphysics Modeling for PWR and VVER Applications", Proceeding International Conference ICAPP 23-27 April 2023 – Gyeongju, Korea
- [16] B. Calgaro, B. Vezzoni, Advanced Couplings and Multiphysics Sensitivity Analysis Supporting the Operation and the Design of Existing and Innovative Reactors, *Energies* 2022, 15(9), 3341; <https://doi.org/10.3390/en15093341>.
- [17] B. Vezzoni, B. Calgaro, A. Brighenti, C. Lafaurie, L. Mercatali, P. Mosca, "Advanced Simulations and Multi-Physics Lattice and Core Modeling for VVER Applications" Proceeding International Conference VVER 2022, ÚJV Řež Conference Centre, Czech Republic, October 10-12, 2022.
- [18] NEA/OECD - Benchmark for Uncertainty Analysis in Best-Estimate Modelling for Design, Operation and Safety Analysis of Light Water Reactors (LWR-UAM)
- [19] F. Acosta et al., "Development and Application of a Novel 3D Neutron Kinetics and Thermal-Hydraulic Coupling Within the ODYSSEE System" The 19th International Topical Meeting on Nuclear Reactor Thermal Hydraulics (NURETH-19) Log nr.: 35691, Brussels, Belgium, March 6 - 11, 2022
- [20] A. Calloo et al., "COCAGNE: EDF new neutronic core code for ANDROMÈDE calculation chain," Proceedings of M&C 2017, Jeju, Korea, April 16-20, (2017).
- [21] Patricot, C., Lenain, R., Caron, D. 2019. Upgraded of APOLLO3@ internal thermohydraulic feedback model with THEDI and application to a control rod ejection accident. M&C 2019. ANS
- [22] Kozłowski, T., Downar, T. 2007. PWR MOX/UO<sub>2</sub> Core Transient Benchmark. Technical Report NEA/NSC/DOC(2006) 20, NEA-OECD. ISBN: 92-64-02330-5. Available at [https://www.oecd-nea.org/science/wprs/MOX-UOX-transients/benchmark\\_documents/final\\_report/mox-uo2-bench.pdf](https://www.oecd-nea.org/science/wprs/MOX-UOX-transients/benchmark_documents/final_report/mox-uo2-bench.pdf)
- [23] Ferraro, D., Valtavirta, V., García, M., Imke, U., Tuominen, R., Leppänen, J., Sanchez-Espinoza, V. 2020. OECD/NRC PWR MOX/UO<sub>2</sub> core transient benchmark pin-by-pin solutions using Serpent/



- SUBCHANFLOW. Annals of Nuclear Energy. Volume 147. 107745. ISSN 0306-4549. <https://doi.org/10.1016/j.anucene.2020.107745>
- [24] Wagner, W., Cooper, J. R., Dittmann, A., Kijima, J., Kretzschmar, H.-J., Kruse, A., Mareš, R., Oguchi, K., Sato, H., Stöcker, I., Šifner, O., Takaishi, Y., Tanishita, I., Trübenbach, J. & Willkommen, T. 2000. The IAPWS Industrial Formulation 1997 for the Thermodynamic Properties of Water and Steam. Journal of Engineering for Gas Turbines and Power. 122. 150-184. <http://dx.doi.org/10.1115/1.483186>
- [25] Ivanov, B., Ivanov, K., Groudev, P., Pavlova, M., Hadjiev, V. 2003. VVER-1000 Coolant Transient Benchmark Volume I: Specifications of the MCP Switching on Problem. Revision 1. NEA/OECD NEA/NSC/DOC.
- [26] NEA/OECD - Benchmark for Uncertainty Analysis in Best-Estimate Modelling for Design, Operation and Safety Analysis of Light Water Reactors (LWR-UAM)
- [27] Fridman, E., Huo X. 2020. Dynamic simulation of the CEFR control rod drop experiments with the Monte Carlo code Serpent. Annals of Nuclear Energy. Volume 148. ISSN 0306-4549. <https://doi.org/10.1016/j.anucene.2020.107707>
- [28] CATHARE3 – Mise en service de CATHARE v2.1.514 sur Cronos – D02-DTIPD-F-21-0389
- [29] AP3 V2.1.1 compilé sur CRONOS  
D02-DTIPD-F-21-0423
- [30] C3PO (Collaborative Code Coupling PlatfOrm)  
Private communication from CEA : C. Patricot, CEA, Septembre 2020
- [31] C3PO Open Source Access  
<https://sourceforge.net/projects/cea-c3po/>
- [32] C. Patricot, "THEDI: a multi-1D two-phase flow solver for neutronic codes", Proceedings of ICAPP2019, Juan-les-Pins, France, May 12-15 (2019).
- [33] Supercalculateurs : le bon calcul pour l'avenir, <https://www.edf.fr/groupe-edf/inventer-l-avenir-de-l-energie/r-d-un-savoir-faire-mondial/les-pepites-de-la-r-d/les-supercalculateurs/supercalculateurs-le-bon-calcul-pour-l-avenir>
- [34] CATHARE-3 V2.1: The new industrial version of the CATHARE code, <https://hal-cea.archives-ouvertes.fr/cea-04087378/>
- [35] CHO, N.Z. KAIST Nuclear Reactor Analysis and Particle Transport Laboratory, Benchmark Problem 1A, <http://nurapt.kaist.ac.kr/benchmark>
- [36] TMI core specifications - <https://www.oecd-nea.org/upload/docs/application/pdf/2019-12/nsc-doc99-8.pdf>
- [37] Bratton, Avramova, Ivanov, Nuclear Engineering and Technology, 2014 - OECD/NEA BENCHMARK FOR UNCERTAINTY ANALYSIS IN MODELING (UAM) FOR LWRS – SUMMARY AND DISCUSSION OF NEUTRONICS CASES (PHASE I), <https://www.sciencedirect.com/science/article/pii/S1738573315301285>
- [38] K. Ivanov, T. Beam, A. Baratta, A. Irani, and N. Trikouros, "PWR MSLB Benchmark. Volume 1: Final Specifications", NEA/NSC/DOC (99)8, April 1999.
- [39] D3.2 6 The CAMIVVER Definition report with specification for NPP with VVER 1000 reactor with respect to selected transients
- [40] VVER-1000 COOLANT TRANSIENT BENCHMARK – PHASE 1 (V1000CT-1) Volume I: Final Specifications (Revision 4) - NEA/NSC/DOC(2002)6
- [41] Y. Bilodid, E. Fridman, T. Lötsch, X2 VVER-1000 benchmark revision: Fresh HZP core state and the reference Monte Carlo solution, Annals of Nuclear Energy, 144 (2020)
- [42] D4.4 deliverable – Results of the verification phases on PWR and VVER geometry configurations.
- [43] Horeka, "High-performanced Computing (HPC)," [Online]. Available: <https://www.scc.kit.edu/en/services/horeka.php>.
- [44] "Serpent Wiki online user manual," [Online]. Available: [https://serpent.vtt.fi/mediawiki/index.php/Main\\_Page](https://serpent.vtt.fi/mediawiki/index.php/Main_Page).

# 1. Introduction

---

The H2020 CAMIVVER project Work Package 5 (WP5) is dedicated to advanced coupled neutronic and thermal-hydraulics calculations for both PWRs and VVERs cores and to benchmarks with advanced codes.

In WP5, three main tasks were established in the project proposal [1] specially conceived to support multiphysics core calculations and advanced couplings developments. Task 5.1 and the associated D5.1 [2] with its consolidated version in D5.2 [3] consists in the definition of the VVER and PWR reduced size core reference test cases with their corresponding initial and boundary conditions. Task 5.2 evaluates steady-state and transient scenarios related to VVER [4] geometries with different core neutronics and channel thermal-hydraulics tools such as APOLLO3®/THEDI and the High-Fidelity SERPENT2/SUBCHANFLOW coupling tool. By making use of the cases defined in Task 5.1, the efforts within Task 5.2 will contribute to the success of Task 5.3 [1] which is mainly devoted to the development of a 3D neutronics-thermal-hydraulics reference calculation based on APOLLO3®/CATHARE3 coupling.

Beside the use of already adopted codes and methods for the design and operation of existing NPP, having access at industrial level to advanced calculation tools as the ones adopted in the framework of the CAMIVVER project, will support Long Term Operation (LTO) strategies and also the design of innovative solutions and concepts.

WP5 is tightly connected to the activities of WP4. Deliverable 4.3 [5] from WP4 provides most of the cores, reflectors, and fuel assemblies geometrical and material descriptions, as well as nominal operating conditions. However, for the purposes of WP5, some of the data (mainly boundary conditions) have been updated and specific recommendations have been introduced and documented in the dedicated D5.2 [3].

This document takes into account the recommendations issued from Task 5.1 related to the VVER and PWR test cases, specifying their geometries, materials, thermophysical properties, transient scenarios (initial/ boundary conditions), and output parameters to be extracted and compared. These transient scenarios were simulated by participants with available multi-physics tools and results contribute to both Tasks 5.2 (mainly oriented to VVER minicore case) and 5.3 (mainly oriented to PWR minicore cases).

In Chapter §2 the context that brings several partners to cooperate in the framework of the CAMIVVER project is briefly described.

In Chapter §3 the objectives of Task 5.2 are briefly presented with the definition of the VVER oriented test case and the main hypotheses associated to the scenario definition and associated boundary conditions are also summarized for both steady-state and transient conditions.

In Chapter §4 the description of VVER proposed modeling and codes adopted by the involved partners are described first, taking a high fidelity coupling such as the SERPENT2/SUBCHANFLOWSCF tool developed by KIT as an example of reference calculation for triangular pitch in hexagonal lattice. The main results of comparison between APOLLO3®/THEDI and SERPENT2/SCF for steady-state and transient are also presented.

## 2. Context of VVER advanced core calculations

---

The European increasing need in decarbonated sources of electricity imposes an increasing attention to Long Term Operation (LTO) strategies for both PWR and VVER type of reactors.

For such challenges it is of primary importance to have access to several full 3D core neutronic codes and coupling tools for consolidating the reactor analyses.

Up to now, specific applications have mainly focused on the improvement of the neutronic modeling (nuclear data, heterogeneity, numerical methods, etc.). However, even if neutronics is the main contribution to the physics phenomena involved in the core analyses during evolution and kinetic transient, the feedbacks coming from coupling with other physics have also to be accounted for.

More in general, current industrial codes and methods need to keep innovation as driving force in order to be able to cope with:

- New reactor designs (e.g. EPR, VVER, SMR, HTR, ...);
- New requirements from Safety Authorities (ASN Guide n°28) [6];
- New cycle-oriented loading strategies (e.g. plutonium multi-recycling);
- New challenges of Long-Term Operation dedicated projects.

For the next decade, an industrial stake is to enhance the codes interoperability and the multi-scales analyses as a solution for improving the single and coupled physical phenomena investigation and resolution for different reactor designs including the innovative ones.

### **3. WP5 task 5.2 main objectives**

---

In the framework of the H2020 CAMIVVER project, Work Package 5 (WP5) analyzes and provides best estimate calculations for VVER and first comparison with high fidelity codes. These results provide a starting point for future industrial level roadmaps of tools and methodologies to be adopted [1].

For the correct progress of the WP5, three main tasks were established in the project proposal [1]. Task 5.1 consists in the definition of the VVER and PWR reduced size core reference test cases with their corresponding initial and boundary conditions. Task 5.2 evaluates the aforementioned steady-state and transient scenarios with coupled neutronics and closed channel thermal-hydraulics tools (mainly APOLLO3®, SERPENT2/SUBCHANFLOW). By making use of the cases defined in Task 5.1 and the results to be obtained in Task 5.2, efforts have been made in Task 5.3 for the development of a 3D neutronics-thermal-hydraulics calculation tool based on APOLLO3®/CATHARE3 coupling [4].

WP5 is tightly connected to the activities of WP4. Deliverable 4.3 [5] from WP4 provides most of the cores and fuel assemblies geometrical and material descriptions, as well as, nominal operating conditions. However, for the purposes of WP5, some of the data has been updated.

The document corresponding to Task 5.1 [2] aims at providing the description of the VVER and PWR test cases, specifying its geometry, materials, thermophysical properties, transient scenarios (initial/boundary conditions), and output parameters to be observed. These transient scenarios will be simulated and intercompared with 3D neutronic codes in task 5.2 and with multi-physics tools in Tasks 5.3.

In deliverable D5.1 [2], transient scenarios are provided for both PWR and VVER. The VVER test case is used as basis for comparison among partners on a small core configuration for testing codes capability to model VVER cores in steady-state and transient.

#### **3.1. Core description**

All the detailed information concerning the fuel assemblies loaded in the small VVER core configuration are provided in D4.3 [5]. The hexagonal fuel, its guide tube with absorbers and central tube pin cells are shown in [5] respectively issued from [2]. Geometry and material specifications are provided here (Figure 1 to Figure 4) with more details on the material isotopic compositions that can be retrieved from D4.3 [5].

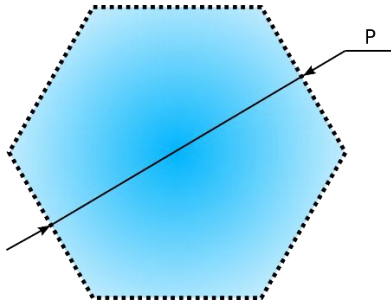


**FIGURE 1 HEXAGONAL UNIT CELL1 (BASED ON [5])**

**TABLE 1 HEXAGONAL CELL PITCH [5]**

Hexagonal Unit Cell	
Unit Cell Pitch (P) [cm]	1.275

**TABLE 2 FUEL PIN CELL GEOMETRY AND MATERIALS [5]**

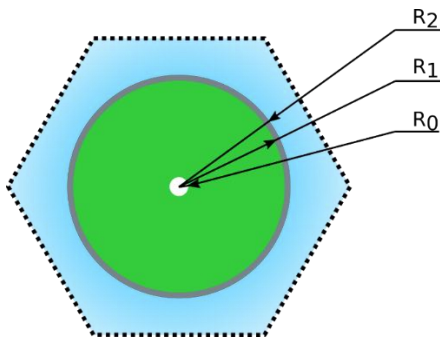


**FIGURE 2 FUEL PIN CELL (BASED ON [5])**

Fuel Pin Cell	
Central void radius ( $R_0$ ) [cm]	0.0750
Fuel pellet radius ( $R_1$ ) [cm]	0.3785
Cladding outer radius ( $R_2$ ) [cm]	0.4550
Fuel pellet material	UO <sub>2</sub> (3.0%, 3.6%, 4.0% <sup>235</sup> U) UO <sub>2</sub> (2.4%, 3.3% <sup>235</sup> U) and 5.0% Gd <sub>2</sub> O <sub>3</sub>
Cladding material	Alloy E110
Void material	Void / He

<sup>1</sup> All images in this section were made with Inkscape [8]

**TABLE 3 GUIDE TUBE AND ABSORBER GEOMETRY AND MATERIALS [5]**

Guide Tube and Control Rod Cell	
Absorber radius ( $R_3$ ) [cm]	0.350
Cladding outer radius ( $R_4$ ) [cm]	0.410
Guide Tube inner radius ( $R_5$ ) [cm]	0.545
Guide Tube outer radius ( $R_6$ ) [cm]	0.630
Absorber material	$B_4C$ or $Dy_2O_3$ $TiO_2$
Cladding material	Steel
Guide Tube material	Alloy E635

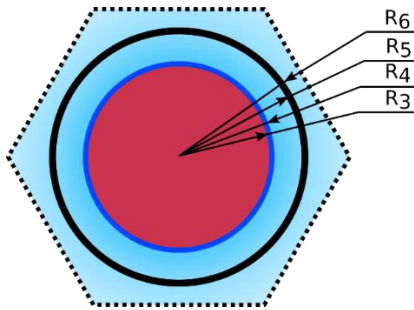


**FIGURE 3 GUIDE TUBE WITH ABSORBER (BASED ON [5])**

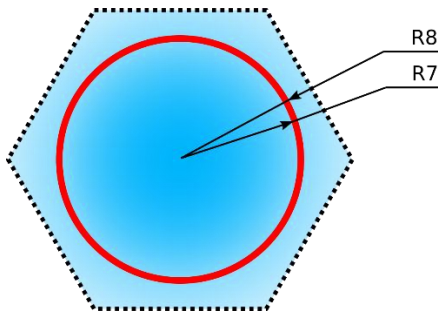


**FIGURE 4 CENTRAL TUBE CELL (BASED ON [5])**

**TABLE 4 CENTRAL TUBE GEOMETRY AND MATERIALS [5]**

Central Tube Cell	
Inner radius ( $R_7$ ) [cm]	0.55
Outer radius ( $R_8$ ) [cm]	0.65
Material	Alloy E635

As far as the PWR minicore, the gap between the fuel pellet and the cladding as well as the one between the absorber and its cladding will not be modelled. Therefore, the cladding thickness is increased in order to fill this gap. Consequently, to keep the mass constant, the Zircaloy is smeared within the volume. The new isotopic composition resulting from this assumption can be found in D5.1 [2].

Two types of fuel assemblies are modelled for the VVER minicore, namely the 30AV5 and the 390GO (Figure 5). The FA lattice pitch is 23.6 cm with a reduced active height of 150 cm instead of 353 cm as reported in D4.3.

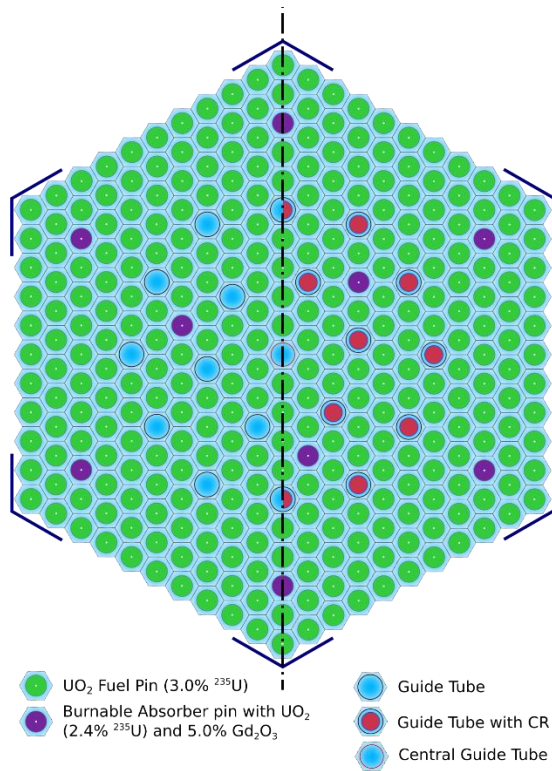


**FIGURE 5: 30AV5 WITHOUT (LEFT) AND WITH (RIGHT) CONTROL RODS (CRS) (BASED ON [5])**

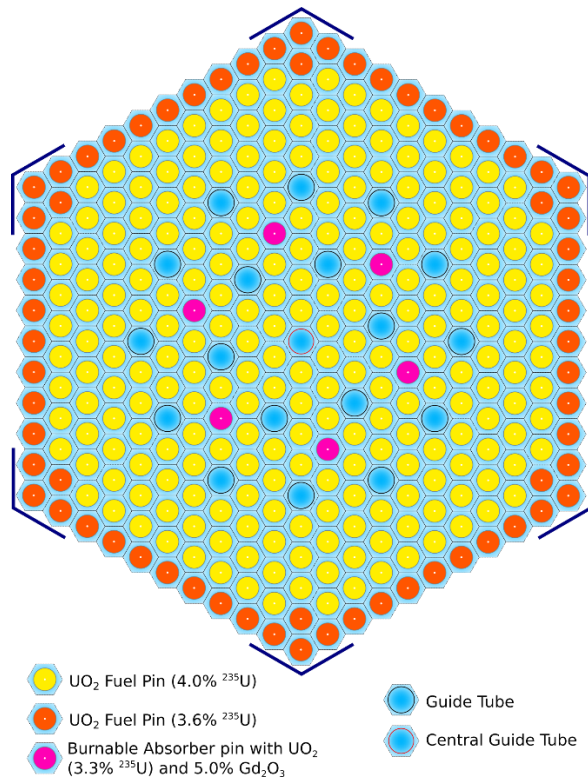


**FIGURE 6 : FUEL ASSEMBLY 390GO WITHOUT CONTROL RODS (CRS BASED ON [5])**

### 3.2. Core description

The VVER minicore layout can be observed in Figure 7. It has seven (7) FAs: one (1) central 30AV5 type FA with the control rods partially inserted surrounded by six (6) 390GO type FAs.

The radial reflector has been modified with respect to its original description in D4.3. In fact the minicore is now surrounded by a layer of borated water with dimensions equal to the FAs pitch.

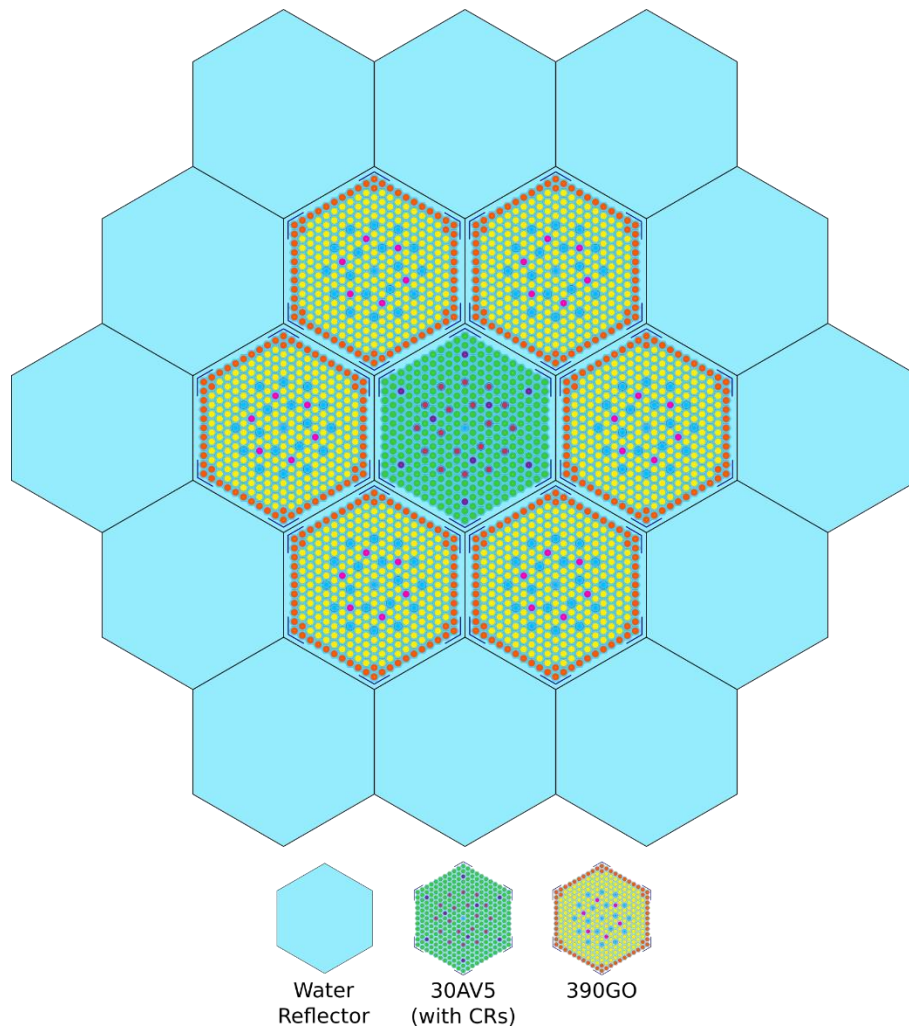


**FIGURE 7: VVER MINICORE LAYOUT (BASED ON [5])**

The top and bottom axial reflectors (30 cm each) are separated into homogenous layers of materials, and they are described by different mixtures of moderator, steel, Alloy E635 and/or Helium [5]. In Figure 8, a schematic of the axial reflector layers can be observed. The thickness of each layer is specified in Table 5 [5] and the material composition is given in D4.3 [5].



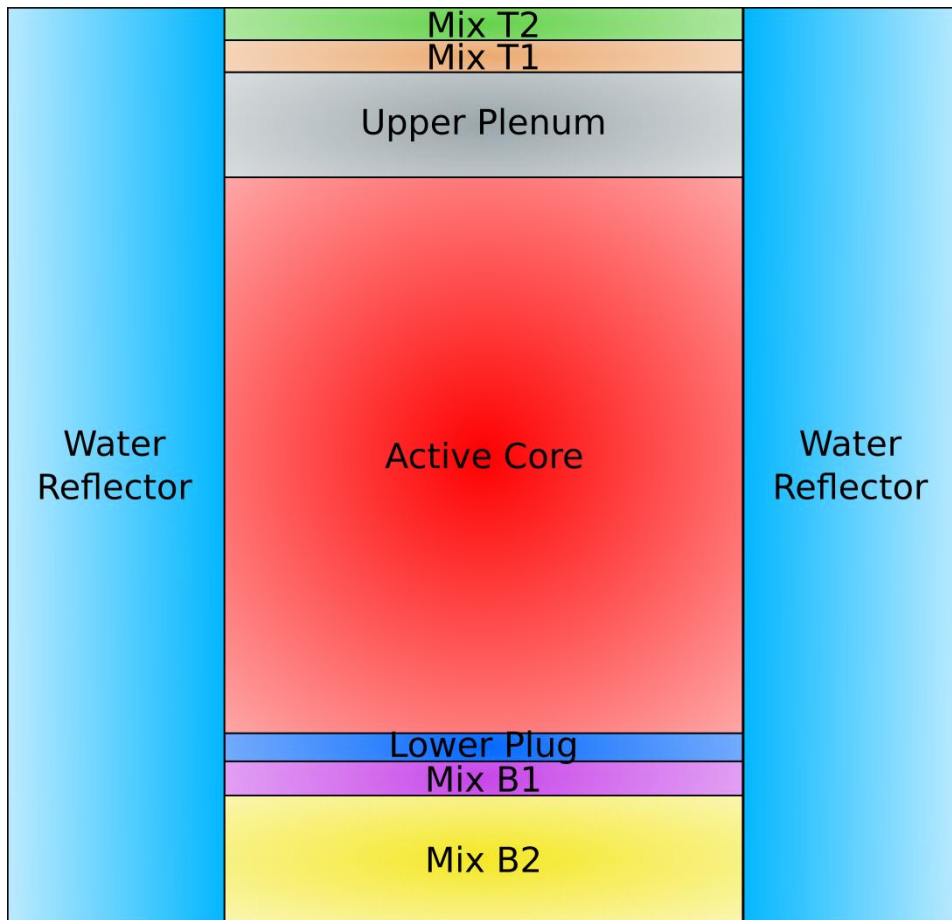


**FIGURE 8: VVER MINICORE RADIAL, TOP AND BOTTOM REFLECTORS (BASED ON [5]).**

**TABLE 5 VVER MINICORE AXIAL DIMENSIONS [5]**

Layer	Thickness [cm]
Mix T2	5.3
Mix T1	4.5
Upper Plenum	22.2
Active Core	150
Lower Plug	2.3
Mix B1	1.7
Mix B2	25

## 4. Transient Scenario

Transient calculations are split into two steps. Firstly, a steady-state calculation is performed at Hot Full Power (HFP) that will serve as the initial condition. Secondly, the transient scenario is simulated with its corresponding boundary conditions and time evolution.

### 4.1.1. Initial conditions

As already mentioned, the initial condition of the transient scenario will be a neutronic-thermal-hydraulics coupled steady-state calculation at the nominal conditions reported in Table 6. Nominal VVER minicore conditions have been provided in [2]. The values in Table 6 are based on realistic full core conditions [26].

In order to confirm the initial hypothesis and to provide intermediate step-by-step comparisons, the initial steady-state before transient has been attained by using High-Fidelity Monte Carlo code before and shared with the partners (Figure 9). At the end of the iteration among partners on the initial conditions, the values in Table 6 have been finally adopted.

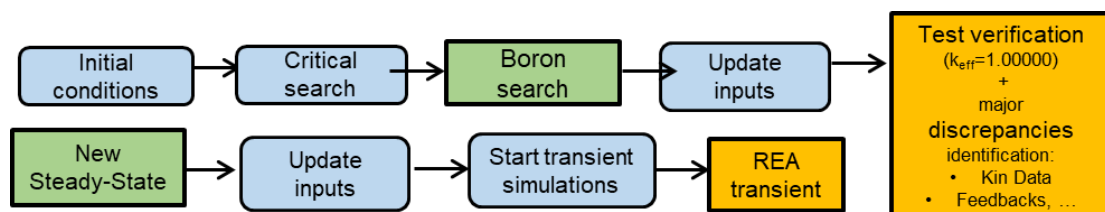


FIGURE 9: INITIAL STEADY-STATE DEFINITION APPROACH

TABLE 6 HOT FULL POWER (HFP) INITIAL CONDITIONS FOR VVER MINICORE [2],[26]

Parameters	Values
Reactor power [MWth]	55
Inlet Water temperature [K]	562.15
Output Pressure [bar]	157
Inlet mass flow [kg/s]	784.5
Control rod position	Partially Inserted (34%)
Rod ejection time	0.08 s
Control rod composition	B <sub>4</sub> C
Boron concentration [ppm]	403
Core Height [cm]	150
Reflectors Height [cm]	Lower = 30 Upper = 30
Thermal properties	See D51 [2]

With the closed-channels codes, the calculation domain is restricted to the active height. Reflector properties (see D4.3 [5]) remain constant during the steady-state and transient calculations.

A boron critical search will be done in this step. Thus, the initial conditions consist in the coupled solution fields set to criticality by adjusting the boron concentration in the moderator.

### 4.1.2. Transient conditions

Two scenarios have been proposed for the transient simulations of WP5: a rod ejection event [2] (Scenario I) and an optional, sudden change of the thermal-hydraulics boundary conditions (Scenario II). The project partners decided to focus on the scenario 1 to investigate it deeply in the limited project time available, before moving to scenario 2 studies that will be considered for a following phase. For the fuel pin thermal calculation, the thermal power is considered generated uniformly over the fuel pellet radius. An equivalent fuel effective temperature is calculated from the radial fuel temperature profile in the fuel pin.

The chosen transient scenario to study consists in a Reactivity Insertion Accident (RIA): starting from HFP conditions and the system critical with boron, the control rod is ejected in 0.08 seconds and the other boundary conditions are kept constant. The rod is moved at a constant velocity to the corresponding position and the system evolution is simulated up to 2 seconds. The aim of this transient scenario is to have a high enough inserted reactivity (compared to  $\beta_{\text{effective}}$ ) to analyze a fast transient, but low enough to always stay as close as possible in monophasic conditions.

For the 7 FA minicore the central rod (CR1) starts from a partially inserted position and it is fully extracted in 0.08 seconds. The initial position is such that when extracted it will cause a reactivity insertion of  $\sim 1.2\%$ .

## 4.2. Output Parameters

For comparing the partners' codes, specific parameters are considered as important outputs as it has been defined in reference [2].

Major quantities of interest investigated are referred as follows:

1. Initial boron concentration, i.e., the boron concentration obtained from the critical search at HFP conditions with and without CRs. Indicated mainly by the reference solution proposed by SERPENT2/SUBCHANFLOW.
2. Evolution over time of the total system power and dynamic reactivity when available. Several reactivity definitions are possible depending on the weighting function used to calculate it. For the sake of simplicity and comparison<sup>2</sup>, the time dependent neutron balance approach will be used [2]. The dynamic reactivity ( $\rho$ ) can be calculated as:

$$k_{\text{eff}}(t) = \frac{\text{gain}}{\text{loss}} = \frac{N(t)}{C(t) + F(t) + L(t) - S(t)} \quad (1) \quad \rho(t) = 1 - \frac{1}{k_{\text{eff}}(t)} \quad (2)$$

---

<sup>2</sup> This approach can be considered as an unweighted calculation (or weighted with an unit-value function). This is to avoid additional calculation of the adjoint function. Eventually, other alternatives can be explored such as the inverse point kinetics method from [27].

Where  $k_{eff}$  is the time dependent neutron balance multiplication factor (neutrons gain-loss ratio),  $N, C, F, L$  and  $S$  are the integrated<sup>3</sup> fission neutron production, capture, fission, leakage and scattering production ( $nxn$  reactions) rates respectively.

Other quantities of interest may be added for further investigations.

---

<sup>3</sup> Integral over space, energy and direction (not time).

## 5. Summary of major results for the 7 FAs VVER test case

---

D5.3 is fully oriented to VVER core modeling with APOLLO3® and in the following the description of WP5 VVER activities that contributes to the consolidation of APOLLO3®/THEDI VVER modeling for both steady-state and transient can be found.

Most of the effort provided by WP5 concerning APOLLO3® core activities were spent mainly to consolidate input decks, pre- and post-processing tools and providing feedbacks on first attempt MPOs delivered by the WP4. Having access to a small core numerical benchmark sufficiently representative of real configurations, was a precious exercise to contribute to the industrialization of the NEMESI automation of APOLLO3® for PWR but also for VVER core modeling (see Figure 10).

The 7 FAs small core was initially described in [5] and all results directly contributes to the task 5.2 as summarized in this deliverable.

Major information concerning the geometry and composition of fuel assemblies is provided in [2].

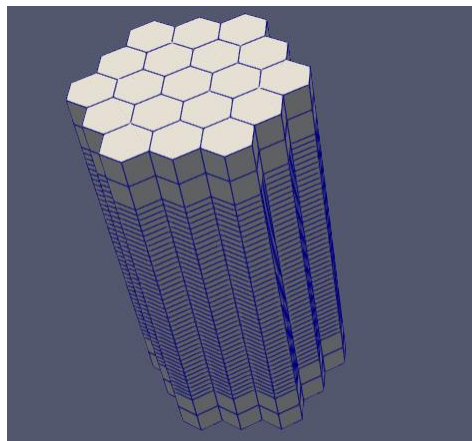


**FIGURE 10: 7 FAS VVER MINI-CORE.**

### 5.1. APOLLO3®/THEDI code description

In the activities carried out within WP5 task 5.2, the APOLLO3® /THEDI core solver has been used. It has been the occasion of testing Python API for PWR and VVER configurations. APOLLO3® is the new generation French deterministic code for lattice and core calculations, developed since 2007 at the CEA with support of EDF and Framatome [9].

A synthetic description of the solvers available for APOLLO3® lattice and core calculations is shown in Figure 11.

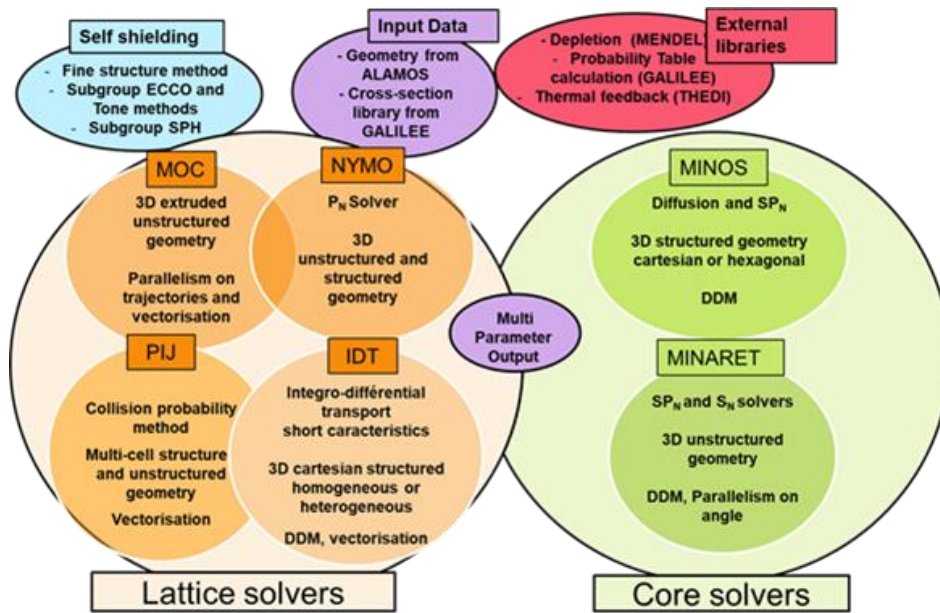


**FIGURE 11: APOLLO3® SOLVER AVAILABLE.**

For the activities carried out in Task 5.2, for core calculations the following options have been used:

- MINOS solver: SP<sub>N</sub> equation on Cartesian and Hexagonal 3D structured geometries using Raviart-Thomas space finite elements,
- Diffusion approximation,
- 2 energy groups calculations,
- Homogeneous assembly XSs.

THEDI is a multi-1D, two-phase flow solver [9]. The main thermohydraulic model is one-dimensional and treats a four-equations system composed of total mass conservation, vapor mass conservation, total motion equation and total internal energy conservation. The core is therefore divided into separated 1D channels sharing consistent boundary conditions: this is the “multi-1D approach”.

The coupling between APOLLO3® and THEDI can be achieved by either using THEDI as an internal library of the APOLLO3® code (approach used in CAMIVVER) or externally using the C3PO coupling kernel.

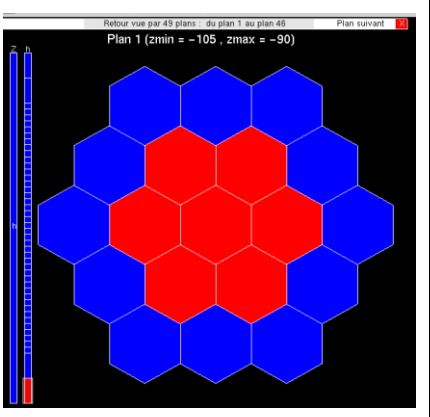
## 5.2. 7 FAs VVER core test case

A short summary of the 7 FAs VVER core benchmark is provided here underling some additional details not yet available in D5.1 [2] (see Table 6 to Table 8) such as:

- Control rod material definition: B<sub>4</sub>C
- Control rod position: intermediate at 51 cm from the top
- Boron concentration = 403 ppm
- Control rod ejection time = 80 ms
- Kinetic data (see Table 8)
- Fresh fuel composition (BU= 0 GWd/tiHM)

**TABLE 7: GEOMETRIC DATA CONSOLIDATION**

Geometrical data consolidation	
Total Flow area [m <sup>2</sup> ]	0.18
Total core cross section area [m <sup>2</sup> ]	0.34
heated perimeter [m]	62.44
wetted perimeter [m]	67.7



As already mentioned, D4.3 and D5.1 do not include kinetic data information. In Table 8 the delayed fractions and the delayed decay constants for 8 families of precursors have been provided based on JEFF3.1.1 data. These data are the ones suggested by KIT (see next section for more information) for the 7 FAs VVER core case.

**TABLE 8: KINETIC DATA FOR THE 7 FAS CORE CASE**

Mini core case	7VVER	
Precursor families	BETA (pcm)	Lambda (1/s)
1	23.3	0.0125
2	109.6	0.0283
3	65.5	0.0425
4	144.3	0.1330
5	245.3	0.2925
6	81.4	0.6665
7	68.2	1.6348
8	25.6	3.5546
<b>Total (1 effective group)</b>	<b>763.1</b>	<b>0.464</b>

### 5.3. The high-fidelity solutions (KIT)

The coupling tool between the neutronic Monte Carlo code SERPENT v2.1.32 [10], and the subchannel thermal-hydraulic code SUBCHANFLOW v 3.7.1 (SCF) [11] has been used as the high-fidelity solution for the rod ejection transient in the 7FAs VVER minicore. The adopted coupling scheme is based on the standard master-slave approach, and extensive literature about the tool can be referred to in [12], [13], and [14]. A description of the neutronic and thermal-hydraulic models is presented in this section.

Figure 12 shows the model developed in SUBCHANFLOW for the 7FA VVER minicore, which consists in a fuel-centered model<sup>4</sup>. A total amount of 2317 rods (7FA x 331) and 2317 channels, both rods and channels divided axially into 30 axial slices (5 cm each axial cell). A MedPreprocessor program developed at KIT allows the creation of the layout geometry for SCF (layout and connectivity files for rods and channels<sup>5</sup>), the IFC<sup>6</sup> files needed by SERPENT2, and the mapping files that link pin-by-pin and channel-by-channel the two domains defined by each code.

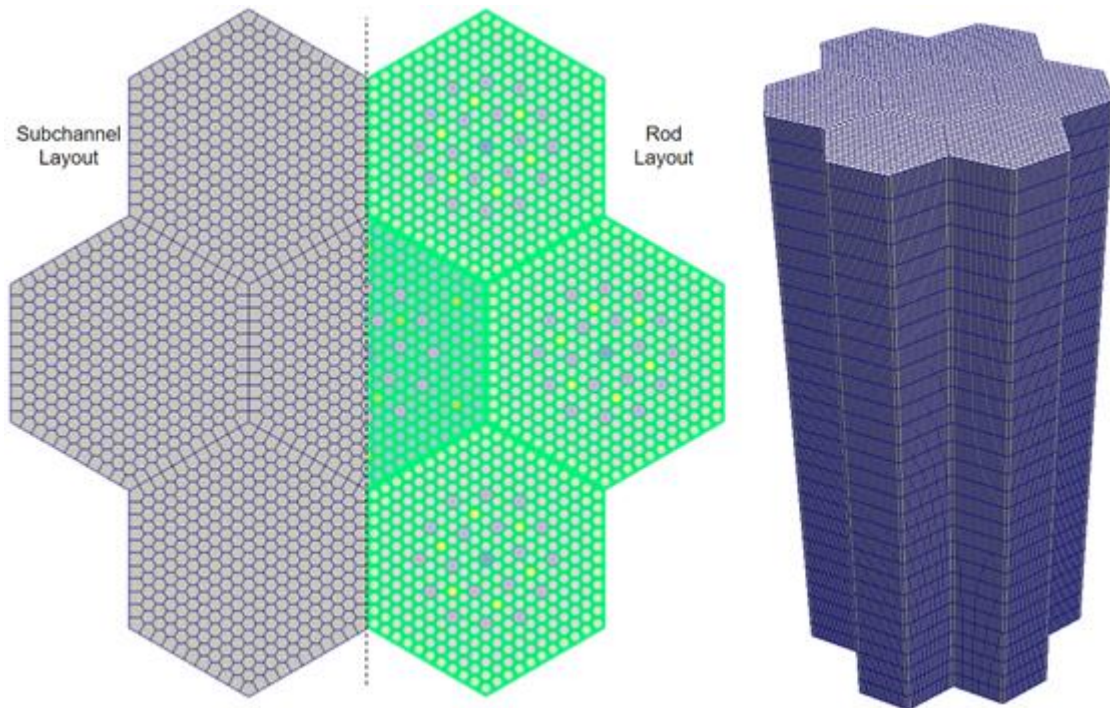


**FIGURE 12. SUBCHANFLOW FUEL-CENTERED MODEL AT PIN/SUBCHANNEL LEVEL.**

Figure 13 shows the full core model developed in SERPENT2 as specified in [2]. Figure 14 shows the fuel IFC file's header, where the feedback takes place in the **UO2** (fuel) material, each fuel assembly is built using 23x23 hexagonal meshes (4<sup>th</sup> and 5<sup>th</sup> lines in yellow, two lines to differentiate the two different FAs). Then fuels are embedded into a 3x3 hexagonal mesh that defines the core (3<sup>rd</sup> line in red) with 30 axial slices. Figure 15 shows the coolant IFC file's header where the feedback occurs in the **wat** (coolant) material. The same hexagonal meshes are considered for the coolant due to the fuel-centered model developed in SUBCHANFLOW. JEFF 3.1.1 nuclear data library is considered.

<sup>4</sup> A rod is surrounded by a channel in a fuel-centered model.

<sup>5</sup> Figures show a graphical representation of the models developed in SUBCHANFLOW. Actually, no hexagonal-shape channels are considered in the model, but information that represents that geometry (e.g. flow area, wetted perimeter, and heated perimeter) is considered for each channel. Peripheral channels of the fuel assembly are bigger than internal channels because some remaining gaps around the assembly have to be considered.

<sup>6</sup> Universal multi-physics interface (IFC) are used in SERPENT2 to easily bring in temperature and density solutions from any external solvers. With the IFC, the solution fields (temperature/density) can be overlaid on top of the base geometry model [43].



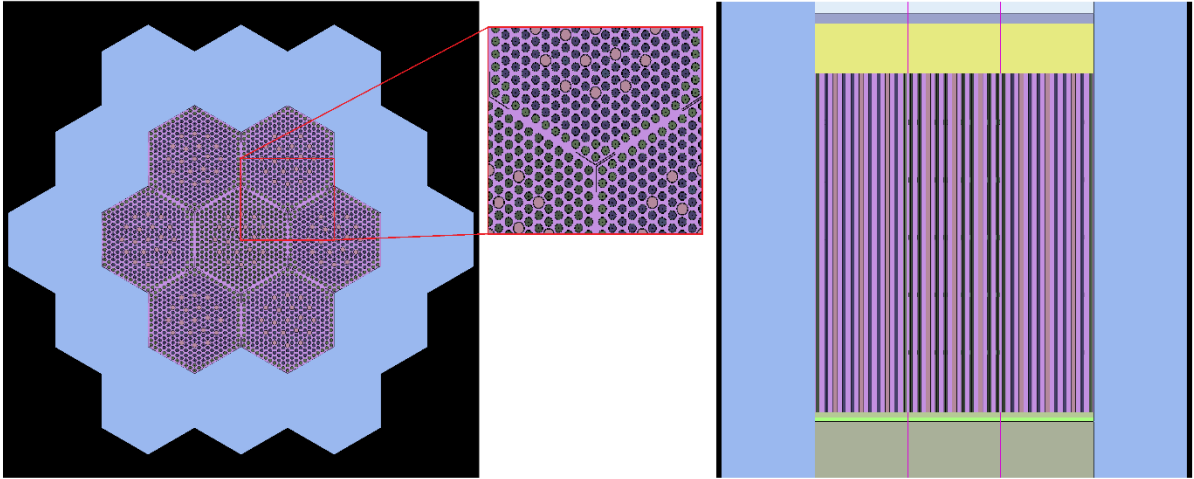


FIGURE 13. RADIAL AND AXIAL SERPENT2 MODEL DETAILS.

```

22 UO2 2 fuel.ifc.out
4
12 4 0.000000e+00 0.000000e+00 2.360000e+01 -7.500000e+01 7.500000e+01 3 3 30
11 5 0.000000e+00 0.000000e+00 1.275000e+00 -1.000000e+18 1.000000e+18 23 23 1
10 5 0.000000e+00 0.000000e+00 1.275000e+00 -1.000000e+18 1.000000e+18 23 23 1
0 5 0.000000e+00 0.000000e+00 1.000000e+18 -1.000000e+18 1.000000e+18 1 1 1

```

FIGURE 14. FUEL IFC FILE'S HEADER

```

22 wat 0
4
12 4 0.000000e+00 0.000000e+00 2.360000e+01 -7.500000e+01 7.500000e+01 3 3 30
11 5 0.000000e+00 0.000000e+00 1.275000e+00 -1.000000e+18 1.000000e+18 23 23 1
10 5 0.000000e+00 0.000000e+00 1.275000e+00 -1.000000e+18 1.000000e+18 23 23 1
0 5 0.000000e+00 0.000000e+00 1.000000e+18 -1.000000e+18 1.000000e+18 1 1 1

```

FIGURE 15. COOLANT IFC FILE'S HEADER.

Doppler temperature with a factor of 0.7<sup>7</sup> is considered for the fuel temperature feedback in SERPENT2. Each fuel pellet is subdivided into ten rings in SUBCHANFLOW to take into account the temperature profiles inside each pellet, and two rings for the cladding. Constant thermophysical properties (e.g. thermal conductivity and specific heat) are considered for the fuel and cladding material, as well as constant fuel-clad gap conductance, and no thermal expansion is considered as specified in [2]. Table 9 shows the main thermal-hydraulic correlations used in the SUBCHANFLOW model.

<sup>7</sup> Doppler temperature is defined as:  $T_{Doppler} = 0.3 \times T_{center} + 0.7 \times T_{outer}$ , where  $T_{center}$  means temperature in the centerline and  $T_{outer}$  is the temperature in the outer surface of the fuel pellet.

**TABLE 9. SUBCHANFLOW CORRELATIONS USED IN THE MODEL**

Correlation	Option selected
Turbulent friction	Blasius
Heat transfer	Dittus Boelter
Critical heat flux	Westinghouse-3
Water Properties	IAPWS-97

The following procedure to get the initial critical steady-state for the transient scenario was followed.

1. Boron and control rod search was performed in a steady-state calculation, which means that TH feedback is taken into account with the boundary conditions specified in [2].
2. With the control rod totally extracted, a boron search to get 1.2% excess reactivity is performed in a steady-state calculation. From this step, a new boron concentration is obtained.
3. With the updated boron concentration, a critical search for the control rod position is performed in a steady-state calculation. From this step, critical steady-state core conditions are completely defined for the transient.
4. An extra steady-state calculation is performed to generate the source terms needed for the transient simulations with SERPENT2. 1E+06 histories divided in 1E+03 cycles with 100 inactive cycles are considered.
5. 5e4 primary particles per batch and MPI are considered for the transient simulations using 10 ms, 5 ms, and 1 ms as time bins.

### **5.3.1. The APOLLO3®-based solutions**

Two approaches for multi-physics solutions have been tested by Framatome and are described:

- APOLLO3®/THEDI core calculations used in order to improve knowledge around the new generation code APOLLO3® core solver when applied to VVER.
- APOLLO3®/CATHARE3 proof of concept developed in CAMIVVER for investigating the thermal-hydraulic core capabilities of the CATHARE3 code, improving knowledge of new code features and providing feedbacks around its usage for multiphysics couplings.

For the steady-state and transient VVER cases analyzed, the multi-parametric cross section libraries have been generated specially for the CAMIVVER project by using APOLLO3® encapsulated in the NEMESI prototype [7]. To succeed a consolidated version of MPOs for VVER geometries and compositions, the last year of the project has been devoted to continuous feedbacks to test and propose modifications to previous tentative MPOs for VVER. Results are still preliminary as the APOLLO3® encapsulated in the NEMESI prototype is still under development and improvements are expected to increase its level of industrialization.

This effort toward industrialization and consolidation of physical results is needed and it should be continued during the follow up of the project.

## 5.4. Results and discussions

In the following paragraphs the comparison of the steady-state and REA transient's solutions generated by KIT and Framatome for the VVER small core test case with the tools previously presented are briefly discussed and summarized.

### 5.4.1. Core reactivity characterization and first steady-state results.

Core reactivity is analyzed using SERPENT2 stand-alone with constant TH data defined in [5], and then thermal-hydraulic (TH) feedback with SUBCHANFLOW is taken into account. Results are presented in Table 10. Without TH feedback, the core has an excess reactivity of  $-978 pcm$ . A gain of  $\sim 1200 pcm$  in reactivity is obtained with TH feedback. Still,  $243 pcm$  of excess reactivity is insufficient to perform the rod ejection transient. Therefore, searches for boron and control rod position are performed. A final boron concentration of  $403 ppm$  and a control rod 65.7%-extracted is considered next for the transient simulation.

TABLE 10. STAND-ALONE AND STEADY-STATE RESULTS.

TH feedback	CODES	CORE STATE	CR extracted position	BORON (ppm)	CORE REACTIVITY (pcm)
NO <sup>8</sup>	SERPENT2	HFP	100 %	600	$-978 \pm 3$
		HFP	0 %	600	$-6754 \pm 3$
YES <sup>9</sup>	SERPENT2/ SUBCHANFLOW	HFP	100 %	600	$243 \pm 3$
		HFP <b>Boron search</b>	100 %	403	$927 \pm 3$
		HFP <b>CR search<sup>10</sup></b>	65.7 %	403	$6 \pm 3$

### 5.4.2. Preliminary analyses of mid-term point comparisons

The steady-state core operating conditions before transient are described in §5.2. These hypotheses are summarized in previous sections.

Core geometrical feature and control rod locations, with the specification of the ejected one, are provided in Table 7.

<sup>8</sup> Nominal conditions ( $T_{cool} = 560K$ ,  $T_{fuel} = 900K$ ,  $\rho = 0.7526 g/cm^3$ ) from Table 1 [5].

<sup>9</sup> Boundary conditions ( $T_{cool}^{inlet} = 562.15K$ ,  $P_{outlet} = 15.7 MPa$ ) from Table 22 [2].

<sup>10</sup> A  $\beta_{eff} = (761 \pm 3) pcm$  is obtained in the critical state. A control rod weight of  $(1.21 \pm 0.02)g$  can be deduced if control rod is extracted from 65.7% initial position.

According to the transient scenario specifications and boundary conditions in the mini-core test case, as described in the previous sections, the CRs are ejected at constant velocity targeting a CR worth of about  $\sim 1.2\%$ .

During the first part of the benchmarking exercise the comparison among CR worth enables the verification of such targeted reactivity insertion. Despite an important difference detected between APOLLO3® based tools and SERPENT2 and to keep the comparison satisfactory even during transient, a penalization on the beta effective has been adopted in order to be as closed as possible to the targeted reactivity insertion. In a way similar way to the PWR case described in detail in D5.4 [4], an extremely rapid exponential power increase is observed. The increase of the fuel temperature first and the decrease of the moderator density subsequently will counteract the reactivity increase with some delay due to the energy deposition mechanisms. At this point also the delayed neutron production will be needed to sustain the chain reaction and consequently the power will decrease until the delayed neutron generation is strong enough to sustain the fission chain again.

The SERPENT2/SCF axially integrated pin-power map distributions normalized to the nominal powers at the steady-state prior to the transient and at power peak time are shown in Figure 16 for the 7 FAs VVER case, in which the power hot spots close to the ejected CRs can be highlighted. The maximum and average statistical uncertainties associated to the pin power calculations is below 3%.

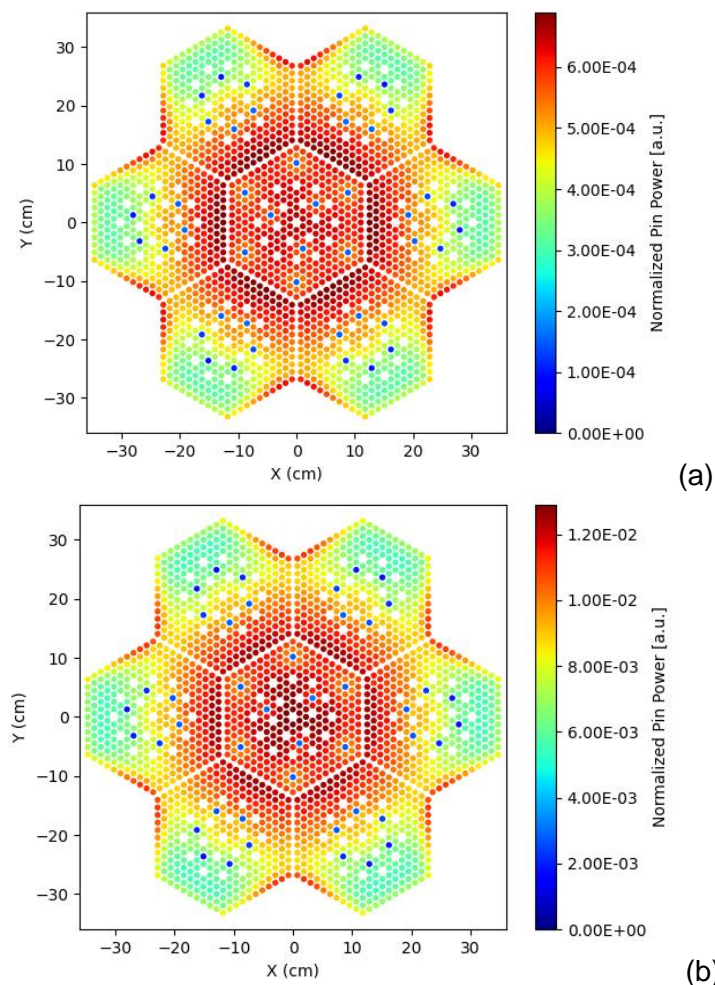


**FIGURE 16: VVER MINI-CORE: SERPENT2/SCF AXIALLY INTEGRATED NORMALIZED PIN RADIAL POWER DISTRIBUTION FOR THE STATE BEFORE THE TRANSIENT (A) AND AT PEAK TIME (B) [15]**

The axial distributions of the center fuel temperature and coolant temperature at power peak times are also provided in Figure 17. This provides an example of the high-resolution capability of the SERPENT2/SCF tools which allows the prediction of reactor fuel and moderator temperature at the local level.

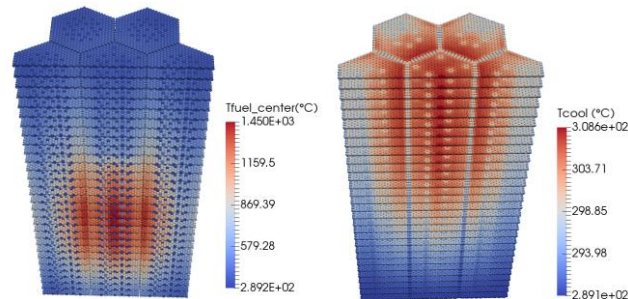


**FIGURE 17: VVER MINI-CORE: SERPENT2/SCF CENTER FUEL TEMPERATURE (LEFT) AND COOLANT TEMPERATURE (RIGHT) DISTRIBUTION AT T=0.12 S [15]**

The first comparisons of the normalized power ( $P/P_0$ ) and reactivity as predicted during the REA transient by APOLLO3@/THEDI and SERPENT2/SCF are shown in Figure 18. A good agreement between the two different solutions can generally be observed.

For the first phase of the transient until the end of the CR ejection at about 0.08 s one can observe an excellent agreement between the reactivity profiles for the 7 FA VVER mini-core. In the second phase of the transient, after the power peak time, some discrepancies can be underlined. This behavior, that may depends on the TH modules and the energy deposition hypothesis (distribution of the energy deposition during transient between fuel pin and coolant), is similar to the one observed for the 32 FAs case (see D5.4 [4]) and confirmed also by the final set of comparison realized during the last part of the project.

As far as the evolution of the normalized power, the shapes of the profiles generated by the different solutions were found to be very consistent one to each other. The peaking values predicted by SERPENT2/SCF are higher with respect to the ones calculated by APOLLO3@/THEDI by ~10% for the VVER (see Table 11).

The power peaks times were also found to be in good agreement within the two solutions, the difference being in the order of ~5 ms (see Table 11).

**TABLE 11 : VVER CASE POWER PEAKING FACTORS AND CORRESPONDING PEAK TIMES PREDICTED BY SERPENT2/SCF, APOLLO3@/THEDI (AP3/THEDI)**

Coupling tool	SERPENT2/SCF	AP3/THEDI
Peak factor [ $P/P_0$ ]	19.55	17.74
Peak time [s]	0.095	0.0895

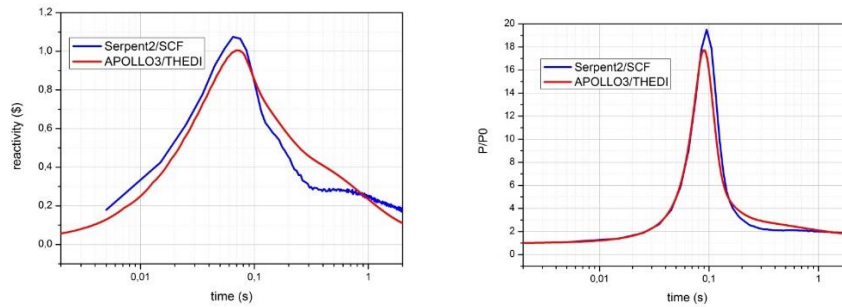


**FIGURE 18: VVER MINI-CORE: REACTIVITY AND POWER EVOLUTION[15]**

### 5.4.3.Last discussions and improvements

During the last months of the project several iterations have taken place on APOLLO3® encapsulated in the NEMESI prototype for VVER applications [7] for adjusting parameters range variations and final debugging of NEMESI. Some version improvements have been also realized in the API interfaces of codes and tools involved in the APOLLO3® based solutions.

Several iterations have been also necessary with WP4 and the development team of the NEMESI APOLLO3® preprocessor to improve the robustness of proposed MPOs for VVER reactor type.

Preliminary results, with a first selection of selected MPOs, have been possible before end 2022 (in line with the milestones fixed at WP4 and WP5) with some improvement in modeling. At assembly level very good agreement was achieved for VVER assemblies between SERPENT2 and APOLLO3® (version 2.3.0dev) as confirmed in WP4 achievements (see details in D4.40), see Table 12.

**TABLE 12 : COMPARISONS SERPENT2/APOLLO3® ON KINF VALUES AT ASSEMBLY LEVEL FOR THE 7 VVER FA CORE**

	APOLLO3® via NEMESI	diff [pcm]
<b>B4C (390GO)</b>	0.99132	-
<b>DY203 (390GO)</b>	1.05496	-165
<b>ARO (390GO)</b>	1.24749	-55
<b>ARO (30AV5)</b>	1.13810	-61

At core level, several sensitivities at boundary conditions, main parameters range variation, transient scenario main options have been tested during the first months of the project as the ones proposed in Table 13.

**TABLE 13 : COMPARISONS BETWEEN APOLLO3® SENSIBILITIES ON STEADY-STATE MAIN CORE PARAMETERS FOR THE 7 VVER FAS CORE**

First results steady-state	APOLLO3® via preliminary sets of FA cross-sections	APOLLO3® via NEMESI 0.1 last 2022
keff	1.05621	1.0569
beta	760	763
Xe	0	0
CR weight [pcm]	888.5	785
CR weight \$	1.17	1.03
CR position from the top [cm]	46	51
bore	<b>400</b>	<b>400</b>
mass flow [kg/s]	4382	4382

As for the 32 FAs core case (D5.4 [4]), a new set of MPOs was realized between the end of 2022 and beginning 2023, accompanied by a cycle of new comparisons at steady-state conditions among SERPENT2/SCF and APOLLO3® at core level.

During the last months of the project a continuous improving of MPOs and modeling options in APOLLO3®/THEDI has been encouraged. In Table 14 the comparison between SERPENT2/SCF and APOLLO3®/THEDI on main core parameters has been realized as well with the very last version of data. Some iterations have been necessary among Framatome, CEA and KIT in order to converge on the very final set of values providing the final results of the CAMIVVER project for the task 5.2.

**TABLE 14 : COMPARISONS BETWEEN LAST VERSIONS SERPENT2/APOLLO3® ON STEADY-STATE MAIN CORE PARAMETERS FOR THE 7 VVER FA CORE ASSEMBLY**

First results Steady-state	SERPENT2/SCF	APOLLO3® MPOs NEMESI Last 2023
<b>Keff</b>	<b>1.00004</b>	<b>0.99127<sup>11</sup></b>
<b>CR weight [pcm]</b>	921	970 <sup>12</sup>
<b>Beta [pcm]</b>	763	763 <sup>13</sup>
<b>Targeted CR weight \$</b>	~1.2	~1.2
<b>CR Pos Top [cm]</b>	51.4	51
<b>Xe</b>	0	0
<b>Bore [ppm]</b>	403	403
<b>mass flow [kg/s]</b>	784.5	784.5

For the VVER case these discrepancies in keff and control rod weight need a deeper analysis that could be carried out in the project follow up.

The keff calculated with the control rod at critical position, with the rodded and with the unrodded conditions at steady-state for both SERPENT2 and APOLLO3® is presented in Table 15.

---

<sup>11</sup> This difference in keff should be investigated deeper. Minor modification since the last final workshop is provided here with agreement in boron concentration comparing Serpent2/SCF and AP3 based tools.

<sup>12</sup> Difference in CR weight at assembly level has been already identified. In the first part of comparisons, a very low penalisation has been adopted for the beta value in order to keep the target ~1.2\$ inserted reactivity. It has been recently verified that for the APOLLO3®/THEDI case this penalization is not necessary. A possible minor discrepancy between CR worth calculation automatic procedure in APOLLO3® as indicated in the table and the value recalculated on the basis of keff has been detected and need further investigations (see for more details Annexe A).

<sup>13</sup> The present version of MPOs generated by WP4 the kinetic data are not included and they are read by the core solver in a dedicated function. The main impact is that the beta effective value is calculated once and remains constant for the whole transient. A modification will be proposed for the follow up of the project.



**TABLE 15 : KEFF COMPARISONS AMONG APOLLO3®/THEDI, APOLLO3® AND SERPENT2 FOR THE 7 FA VVER CORE**

keff	BORON concentration equal to 403 ppm
APOLLO3®/THEDI	Critical rod height = 0.99127 Unrodded =1.00089
SERPENT2	Critical rod height = 1.00006 unrodded = 1.00936

On the basis of the mentioned input configurations, the transient scenario defined in CAMIVVER task5.1 [2] has been simulated. In Figure 19 and Figure 20 transient behavior for normalized power (P/P0) and reactivity indicated in (\$) as predicted during the REA transient by APOLLO3®/THEDI and SERPENT2/SCF are shown. A quite good agreement between the different solutions of the transient can be highlighted.

Spending few words in describing the proposed results it should be mentioned that for both approaches, SERPENT2/SCF and the APOLLO3®/THEDI, two different sets of solutions have been proposed with a major modification proposed (see Appendix A):

- Serpent\_SCF: first batch of results for SERPENT2/SCF, Serpent\_SCF\_23: last batch of results.
- AP3\_THEDI\_7FA: first batch of results for APOLLO3®; AP3\_THEDI\_7FA\_no\_penalisation: last batch of results.

As observed also for the 32 FAs core case (see details in D5.4 [4]), in the second phase of the transient, after the power peak time, some discrepancies persist even after having double checked the thermal properties. The consistency in the different approaches proposed for the definition of the energy fraction deposited in the fuel should also be checked. This point will be investigated during the follow-up of the project and internal R&D activities.

Moreover, the radial and axial discretization are not the same with an APOLLO3® neutronic flux modeling realized with homogeneous assembly mesh approach.

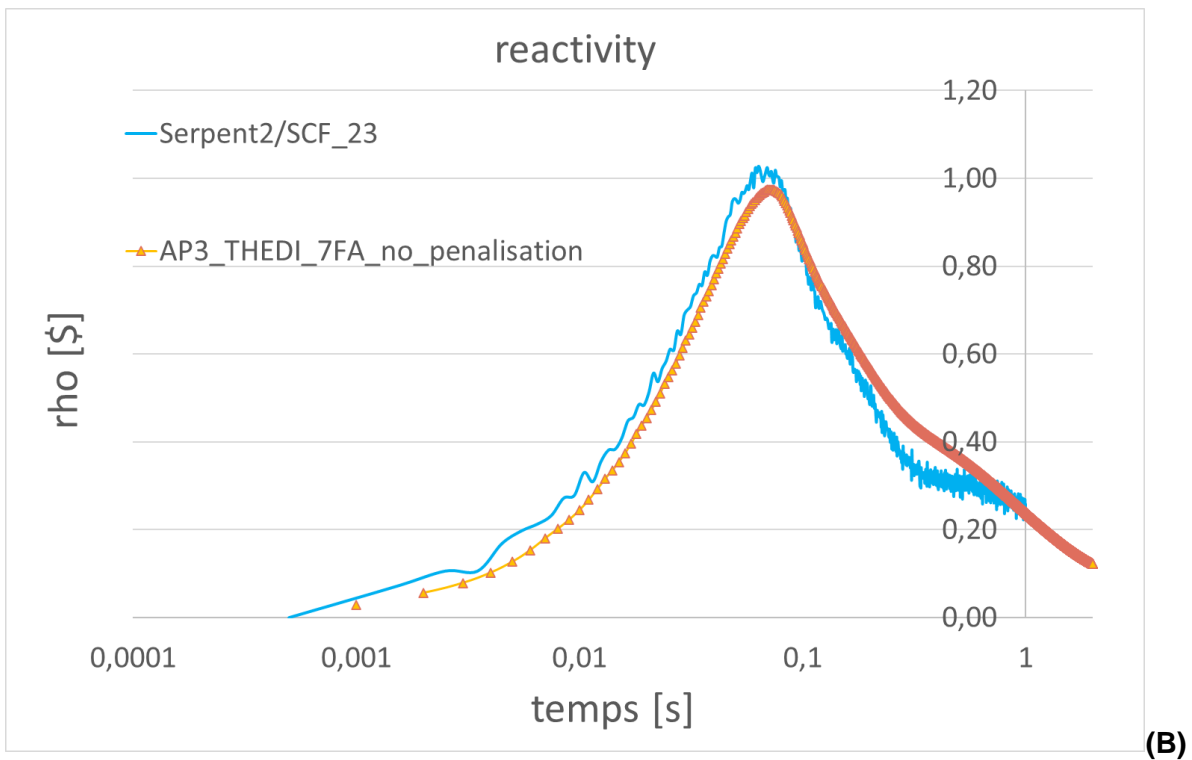
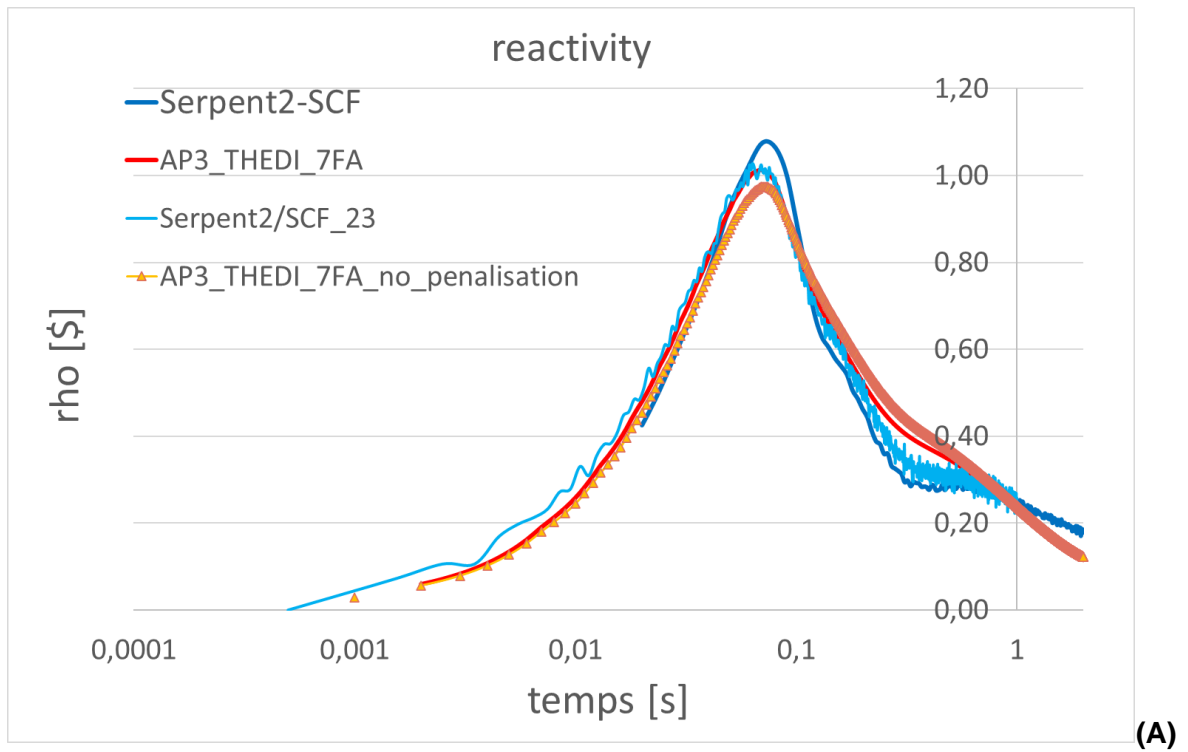


**FIGURE 19: 7 FAS VVER MINI-CORE: LAST COMPARISON REACTIVITY TRANSIENT WITH FIRST AND FINAL RESULTS (A) AND A ZOOM ON FINAL RESULTS (B).**

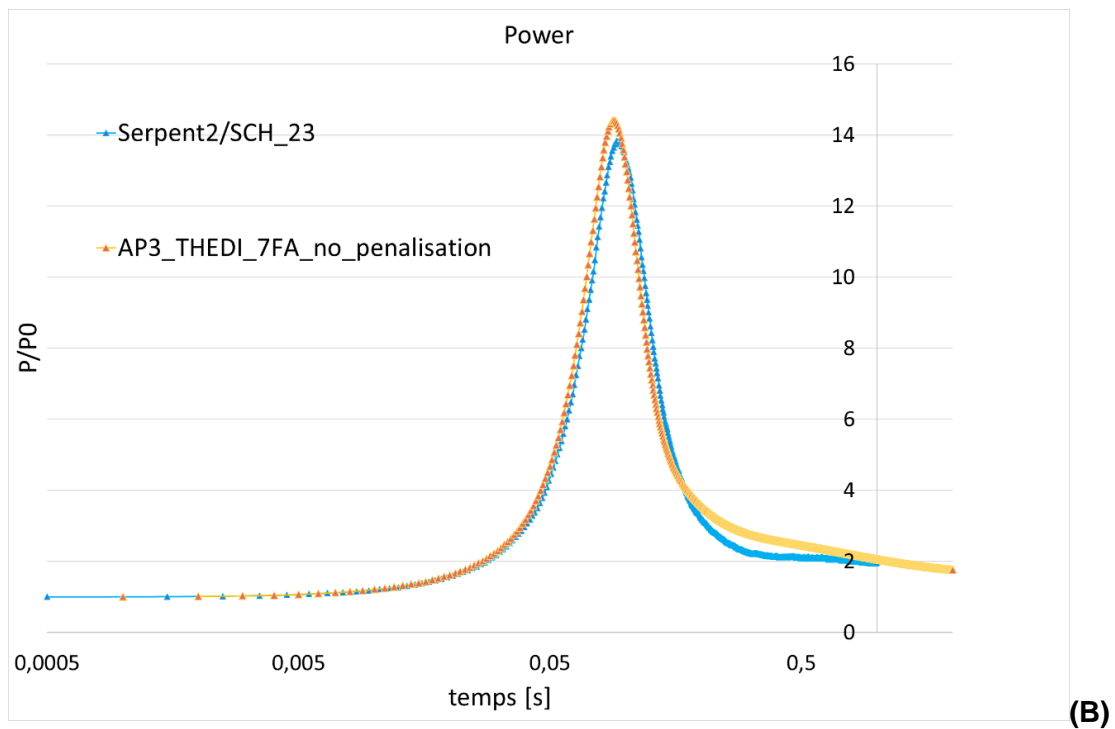
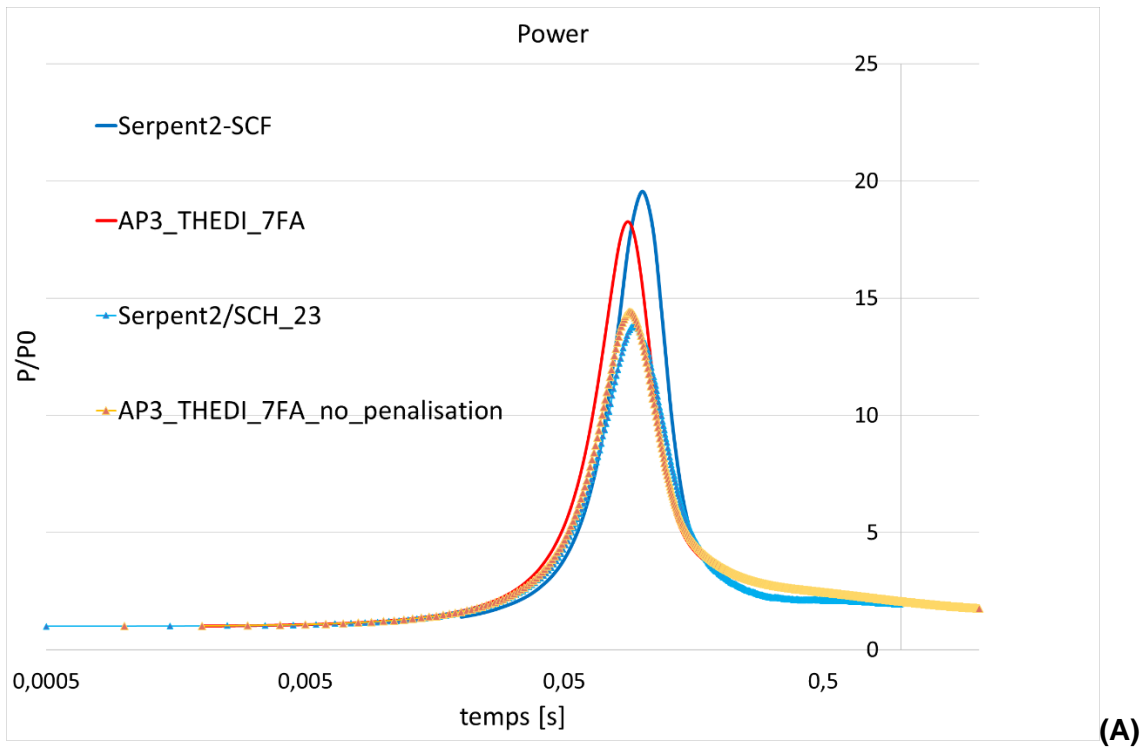


**FIGURE 20: 7 FAS VVER MINI-CORE: LAST COMPARISON POWER TRANSIENT WITH FIRST AND FINAL RESULTS (A) AND A ZOOM ON FINAL RESULTS (B).**

The POC of APOLLO3®/CATHARE3 coupling [15] developed for PWR applications and described in D5.4 [4] has been extended to VVER geometries too. The results obtained on the 7 FA VVER case for the prediction of the power evolution during the REA transient are presented in D5.4 in continuity with PWR mini-core case ones [4].

Several sensitivity analyses have been carried out by KIT with SERPENT2/SCF. The additional results obtained are presented in Appendix B

## 6. Conclusions

---

This document constitutes the deliverable D5.3 of the CAMIVVER project.

It is mainly dedicated to present APOLLO3® core solver based solutions and tools gathered during these years to perform calculations and benchmarks with APOLLO3®/THEDI simplified coupling approach.

All comparisons with SERPENT2 stand-alone or coupled with SCF (KIT) [15] shows an acceptable agreement for steady-state and REA transient even though for a first exercise different radial discretization have been adopted between SERPENT2 (pin-by-pin) and APOLLO3® models (homogeneous on assembly). The results presented in this deliverable are first results and some discrepancies have been underlined and explicated. Further improvements axes have been identified and they will be addressed in the follow-up of the project.

Mainly this activity contributes to an increasing number of APOLLO3® core users from the Industrial partners (namely framatome) and a global skills enhancement on the code. This has allowed to providing feedbacks not only at core level but also at lattice level for what concern MPOs generated by WP4. Even if the distance from APOLLO3® industrialization is still important, the CAMIVVER project confirmed the feasibility of adopting such a code for VVER NPP core modeling.

### 6.1. Perspectives

APOLLO3® core code needs to be extensively tested and used by experienced users with industrial vision to improve its deployment up to a final industrial level. Nevertheless, main functionalities are already available for static and transient analyses, compatible with both cartesian and hexagonal fuel assembly geometries.

A user friendly interface (IHM) is still missing and important work has to be done in order to automatize preprocessing and post-processing asking for improvements in input and output options.

The scenarios proposed here started and facilitated discussions among partners and ease the verification process, but those efforts need to be continued further in the project follow-up.

Fuel assemblies geometry and multi-parametric data libraries MPOs have been an input option from WP4 and WP5 provided feedbacks to WP4 developers. Such interaction is vital for benchmarks success and confirm the need of a global vision in order to judge of codes quality

During last project years, 2022 and 2023, first comparison with High-Fidelity Monte Carlo based resolutions and results from partners were expected in steady-state, possibly evolution and transient conditions. This object purpose was globally attained.

An improvement of accident procedures is for these purposes expected too.

## **Appendix A : APOLLO3 CR worth sensitivity analysis**

---

Some evolution in solutions proposed for both SERPENT2/SCF and APOLLO3®/THEDI have been proposed.

Such evolutions during the CAMIVVER project duration are justified by improvements in MPOs definition, modifications in input options and boundary conditions definitions, bug detection on the codes, increasing code knowledge, etc.

For the APOLLO3®/THEDI case it has been recently verified that the beta effective penalization, initially identified on the basis of the comparison among CR worth differences between S2/SCF and APOLLO3®, took two different values. In the last version of calculation, the results were obtained without penalization. A possible minor discrepancy between CR worth calculation automatic procedure in APOLLO3® and a hand-made calculation based on Keff has been detected and need further investigation.

## Appendix B: SERPENT2/SCF sensitivity analysis and additional results

A sensitivity analysis related to the time bins was carried out in the last months of the project and is presented in this section. In transients, time bins are used in SERPENT2 for population control, but it also affects the time steps in SCF and, of course, the number of times thermal-hydraulic parameters are updated via the coupling in the neutronic code. Table 16 presents the three cases analyzed, which mainly differ in the time bins selected for the transient problem. For case C, more primary particles are considered to increase the statistics of the results.

**TABLE 16. CASES CONSIDERED FOR THE SENSITIVITY ANALYSIS.**

Case	Primary particles	Batch	Number of MPI	Primary particles/batch/MPI	Time bin
A	1E+07	10	20	5E+04	10 ms
B	1E+07	10	20	5E+04	5 ms
C	4E+07	20	20	1E+05	1 ms

Figure 21 presents the core reactivity evolution in time for the three cases, no big differences are observed in terms of reactivity, but more details can be observed with the lower time bin, especially just before the control rod going totally extracted (represented in the plots as a vertical red line at 80 ms). It can be observed that reactivity starts to drop at 70 ms, which means that TH feedback is starting to take into account, as can be observed in Figure 25 and Figure 26 from 40 ms to 80 ms. The starting increase of the fuel temperature is transferred to the neutronic code 1, 2, and 10 times respectively for cases A, B and C, which explains again the starting drop in reactivity and therefore the core power evolution, as observed in Figure 22. Mainly the peak power value is affected, which in case C is ~9% lower than case A. Peak values are summarized in Table 17.

**TABLE 17. PEAK VALUES OBTAINED DURING THE TRANSIENT.**

Case	Peak Reactivity (pcm)	Time bin at Peak Reactivity (s)	Relative Peak Power	Time bin at Peak Power (s)
A	791 ± 3	[0.06-0.07]	15.2 ± 0.2	[0.09-0.10]
B	783 ± 5	[0.070-0.075]	14.4 ± 0.2	[0.090-0.095]
C	786 ± 5	[0.065-0.066]	13.9 ± 0.1	[0.094-0.095]

Regarding uncertainty results, Figure 21 shows that shorter time bins increase uncertainty because fewer particles are simulated in shorter time bins. In the case of C, the number of particles was increased to get better statistics. Figure 23 and Figure 24 show the radial power

distribution at the beginning and at peak power time of the transient for case C, with their respective uncertainty distribution.

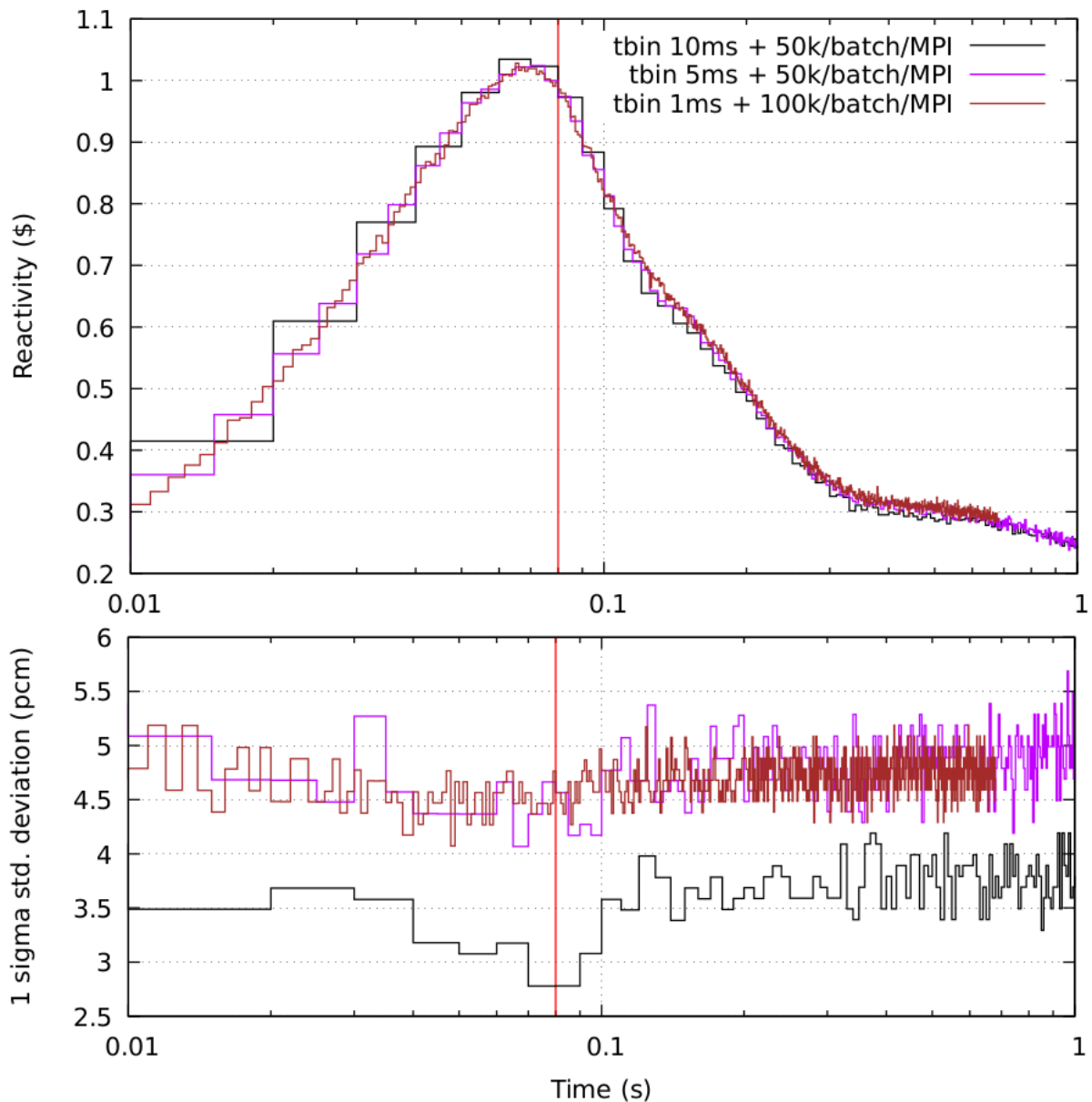


**FIGURE 21. (TOP) CORE REACTIVITY EVOLUTION IN TIME<sup>14</sup>. (BOTTOM) STANDARD DEVIATION ASSOCIATED TO THE MONTE CARLO SIMULATION. VERTICAL LINE MARKS THE TIME WHEN CONTROL ROD IS TOTALLY EXTRACTED.**

<sup>14</sup> Constant  $\beta_{eff}$  of 761 pcm obtained in the initial critical steady-state calculation is used to express reactivity in dollars.

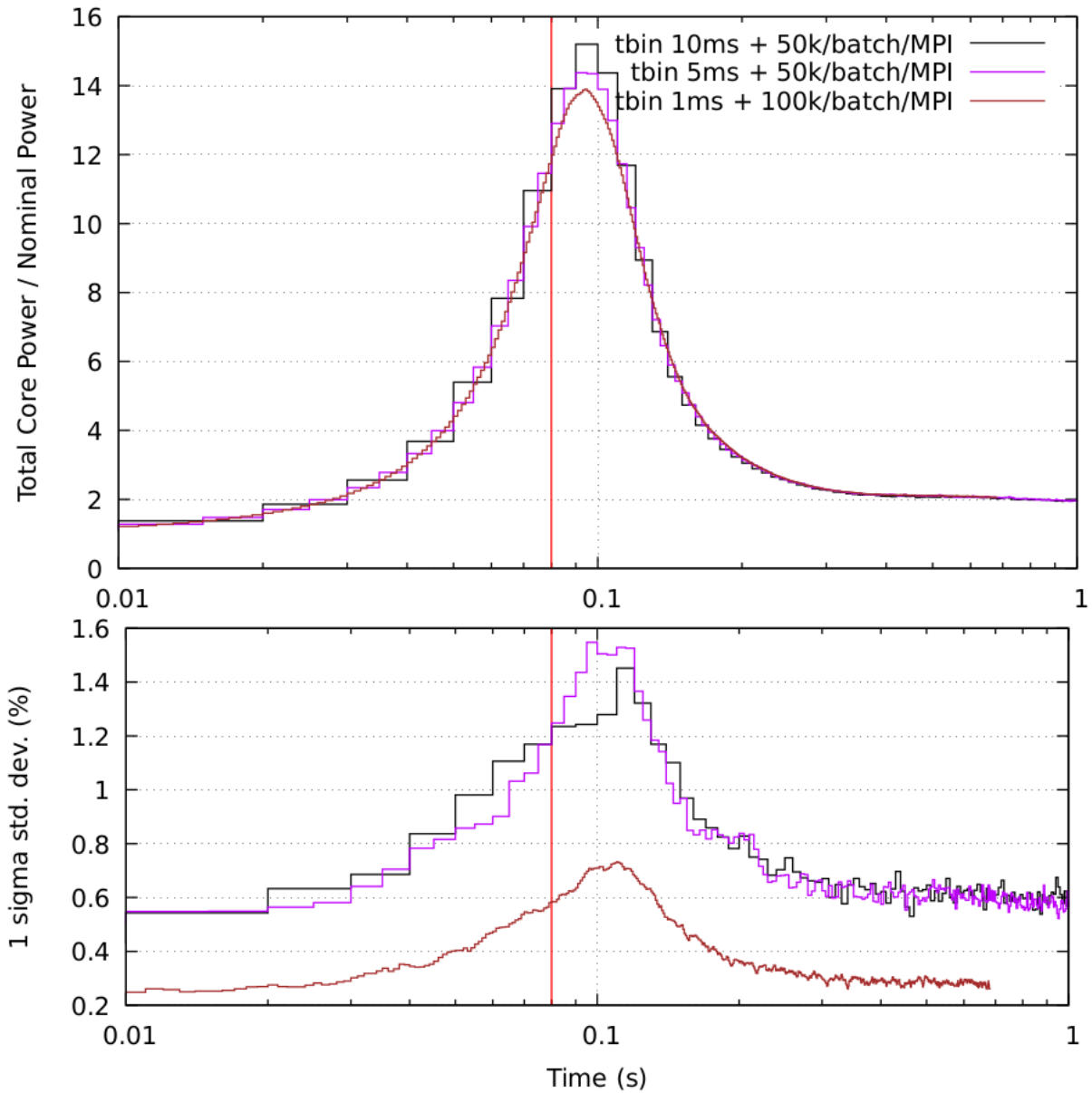


**FIGURE 22. (TOP) NORMALIZED CORE POWER EVOLUTION IN TIME. (BOTTOM) STANDARD DEVIATION ASSOCIATED TO THE MONTE CARLO SIMULATION. VERTICAL LINE MARKS THE TIME WHEN CONTROL ROD IS TOTALLY EXTRACTED.**



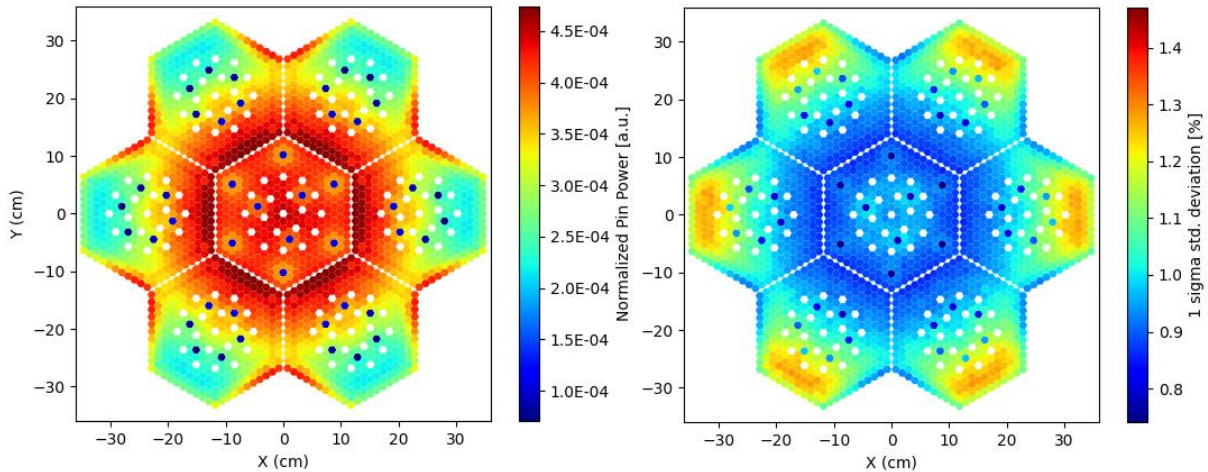


**FIGURE 23. (RIGHT) AXIALLY INTEGRATED NORMALIZED PIN POWER BEFORE THE TRANSIENT IN CASE C. (LEFT) AXIALLY AVERAGED 1 SIGMA STANDARD DEVIATION.**

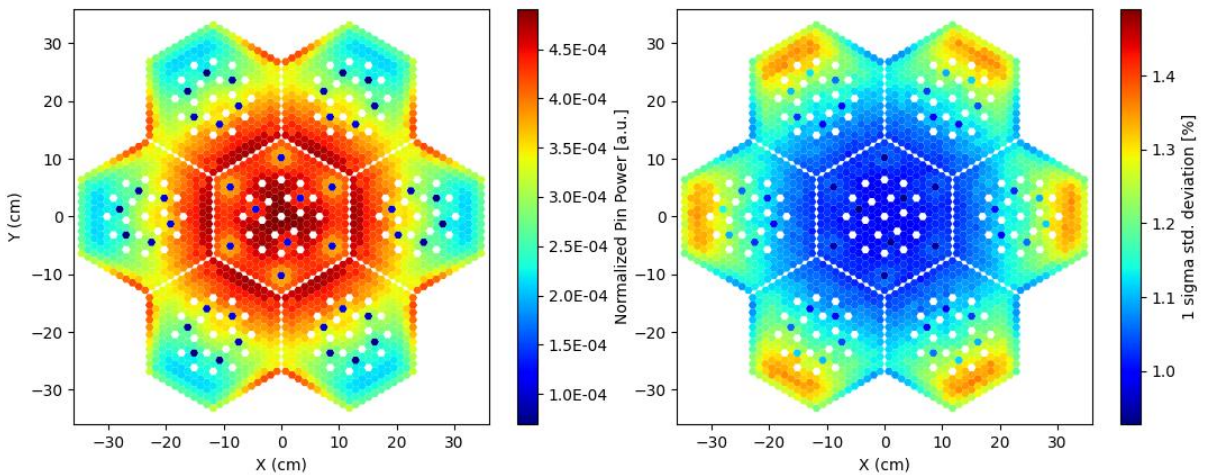


**FIGURE 24. (RIGHT) AXIALLY INTEGRATED NORMALIZED PIN POWER AT PEAK TIME FOR CASE C. (LEFT) AXIALLY AVERAGED 1 SIGMA STANDARD DEVIATION.**

As explained in the model section, 2317 rods and 2317 channels are simulated, each divided into 30 axial slices, leading to 69510 rod-zones and 69510 channel-zones, respectively. Some thermal-hydraulic parameters are selected from that level of detail, and maximum or critical values are presented in the following figures<sup>15</sup>. Figure 25 and Figure 26 show the maximum fuel temperature evolution in the centerline and on the pellet's outer surface. Fuel temperature increases even before the control rod goes totally extracted, inserting negative reactivity into the system and counter-resting the supercritical state. The fuel temperature increases initially very fast up to  $\sim 150$  ms, then a change in the slope is observed because the coolant starts to remove the heat generated in the fuel rods, and therefore coolant temperature starts to increase, as can be observed in Figure 30. Figure 27 shows the fuel temperature map distribution at the beginning and at  $0.682$  s<sup>16</sup> of the transient for case C.

<sup>15</sup> TH parameters for cases B and C were pretty similar, so it was decided only to present case A and C results.

<sup>16</sup> Due to wall-clock time limitations of the KIT-Horeka cluster, simulation was only possible up to  $0.682$  s for case C.

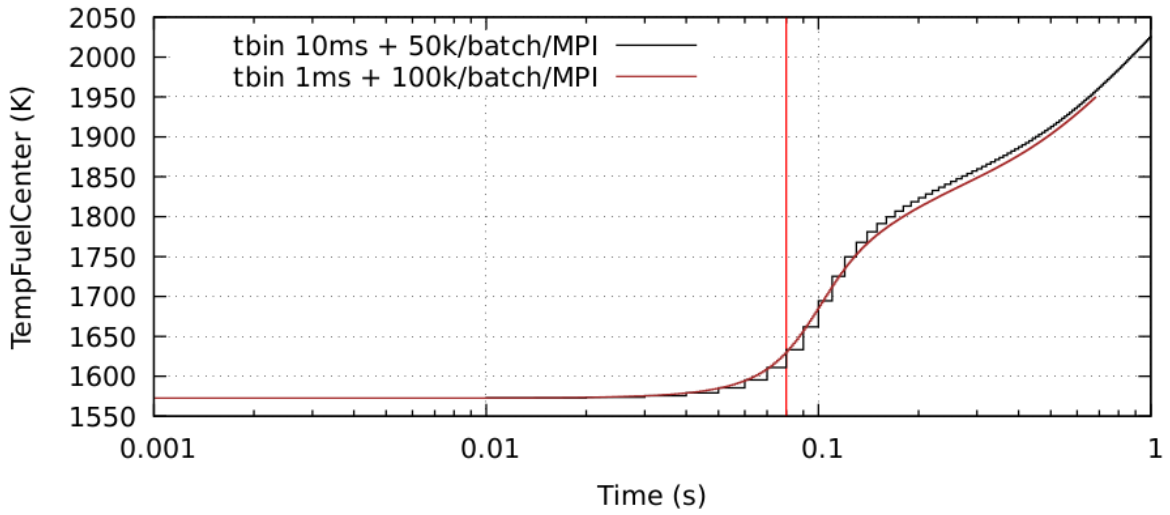


**FIGURE 25. MAXIMUM CENTERLINE FUEL TEMPERATURE EVOLUTION IN TIME.**

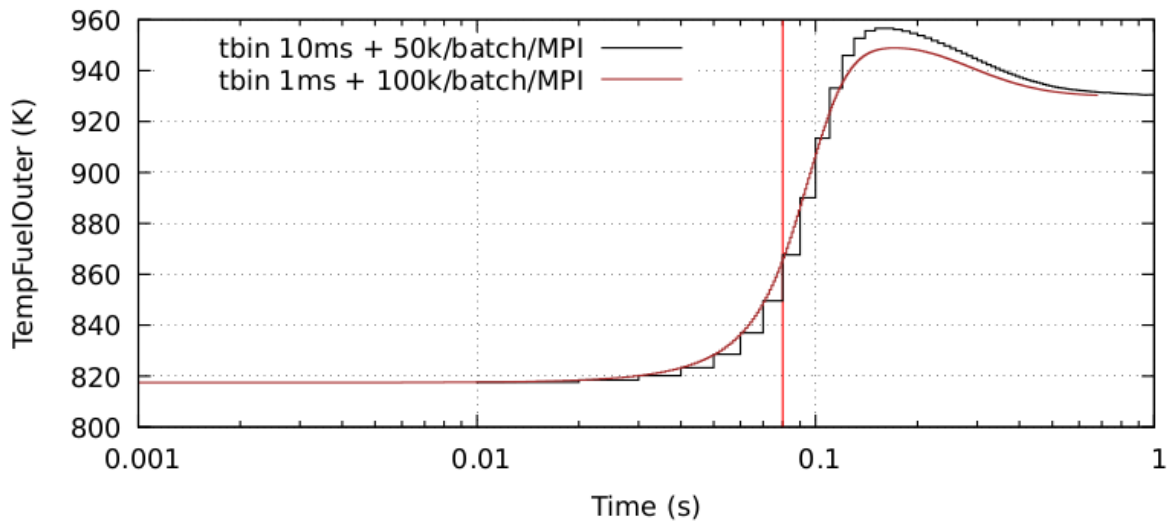


**FIGURE 26. MAXIMUM OUTER SURFACE FUEL TEMPERATURE EVOLUTION IN TIME.**

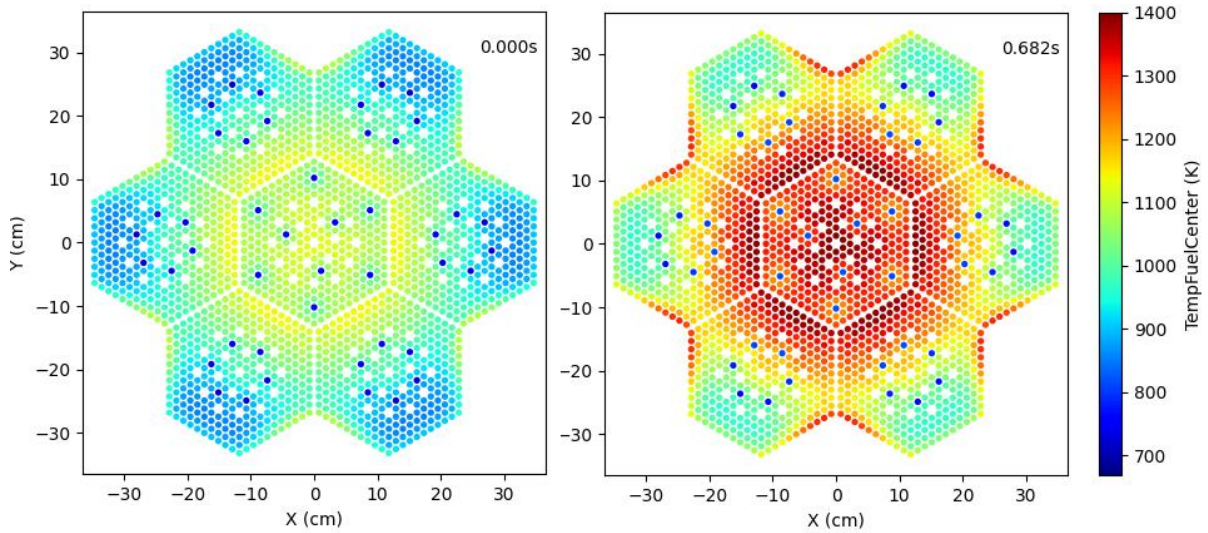


**FIGURE 27. ROD AXIALLY AVERAGED CENTERLINE FUEL TEMPERATURE BEFORE AND AT 0.682 SECONDS OF THE TRANSIENT (CASE C).**

Figure 28 and Figure 29 show the maximum cladding temperature evolution on the inner and outer surfaces. Similar behavior as the fuel temperature is observed for the cladding. The quick increase in temperature is stopped due to the transmission of the heat into the coolant.

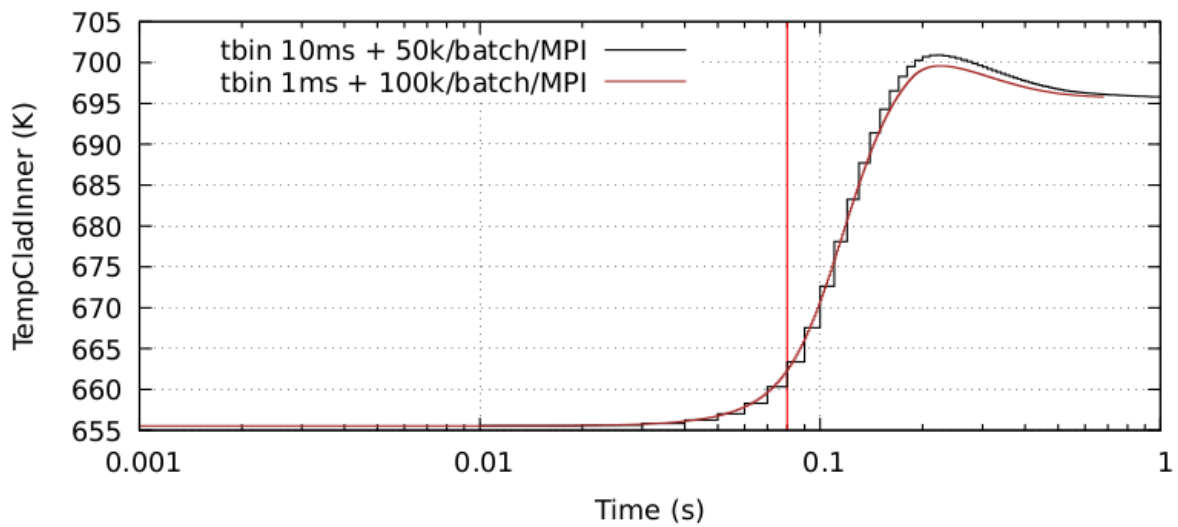


**FIGURE 28. MAXIMUM INTERNAL SURFACE CLADDING TEMPERATURE EVOLUTION IN TIME.**

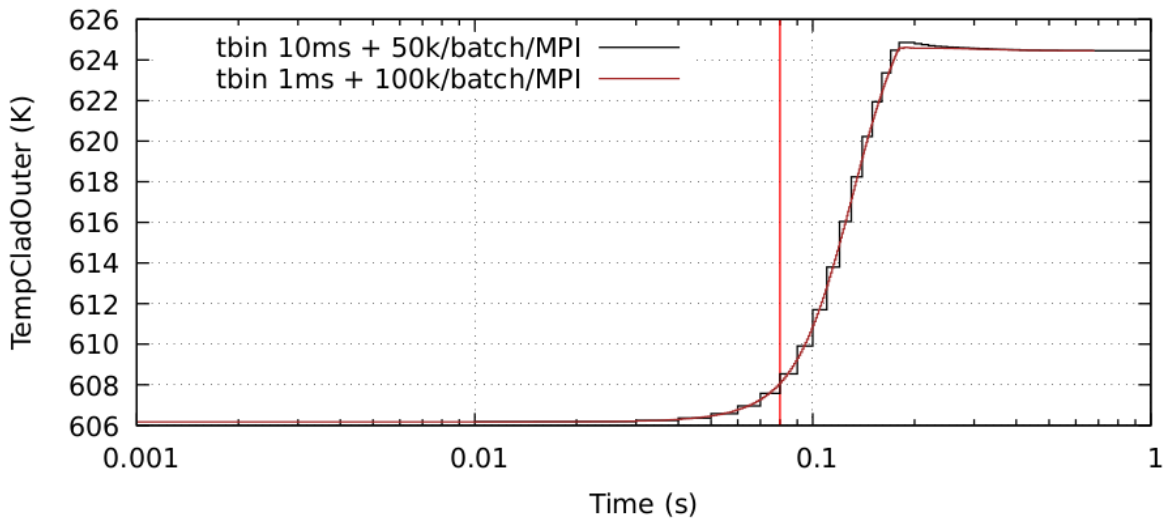


**FIGURE 29. MAXIMUM EXTERNAL SURFACE CLADDING TEMPERATURE EVOLUTION IN TIME.**

Figure 30 shows the maximum coolant temperature evolution in time. No significant differences between cases A and C. As mentioned before, coolant temperature increases at  $\sim 150\text{ ms}$ , removing the heat generated in the pellets and inserting extra negative reactivity into the system. An increase of  $\sim 12\text{ K}$  is observed in the maximum coolant temperature. Figure 31 shows the coolant temperature radial distribution at the beginning and at  $0.682\text{ s}$  of the transient for case C. Lastly, minimum DNBR (departure from nuclear boiling ratio) evolution in time is presented in Figure 32. The minimum value obtained during the transient is 2.64 for case C and W-3 correlation.

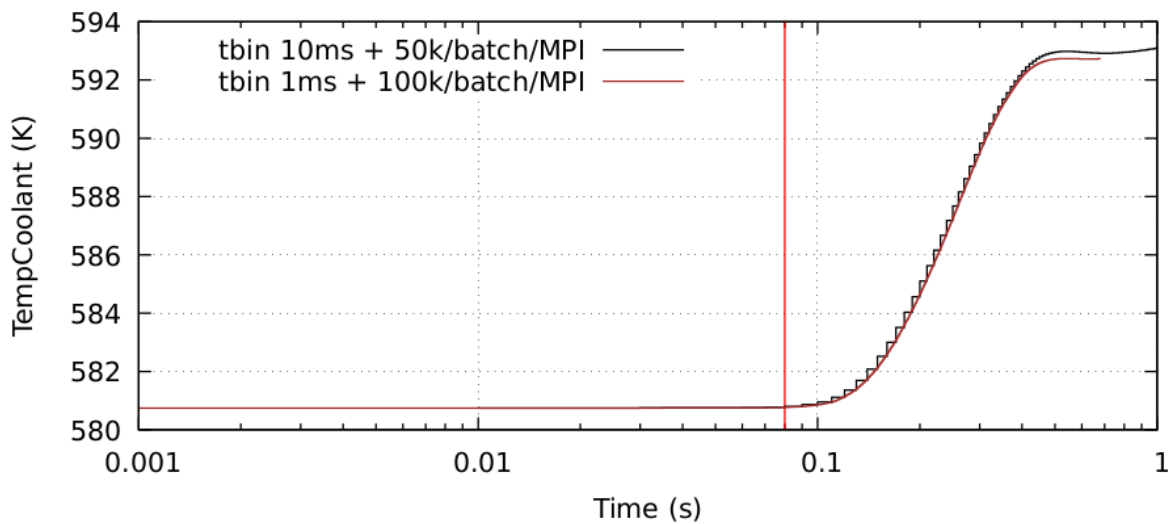


**FIGURE 30. MAXIMUM COOLANT TEMPERATURE EVOLUTION IN TIME.**

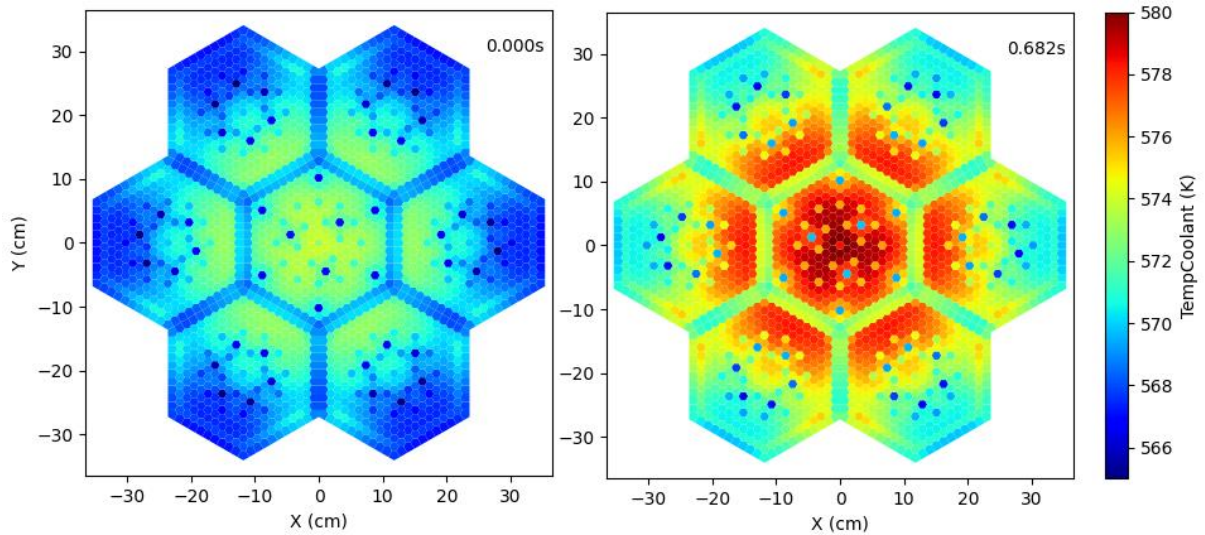


**FIGURE 31. SUBCHANNEL AXIALLY AVERAGED COOLANT TEMPERATURE BEFORE AND AT 0.682 SECONDS OF THE TRANSIENT (CASE C).**

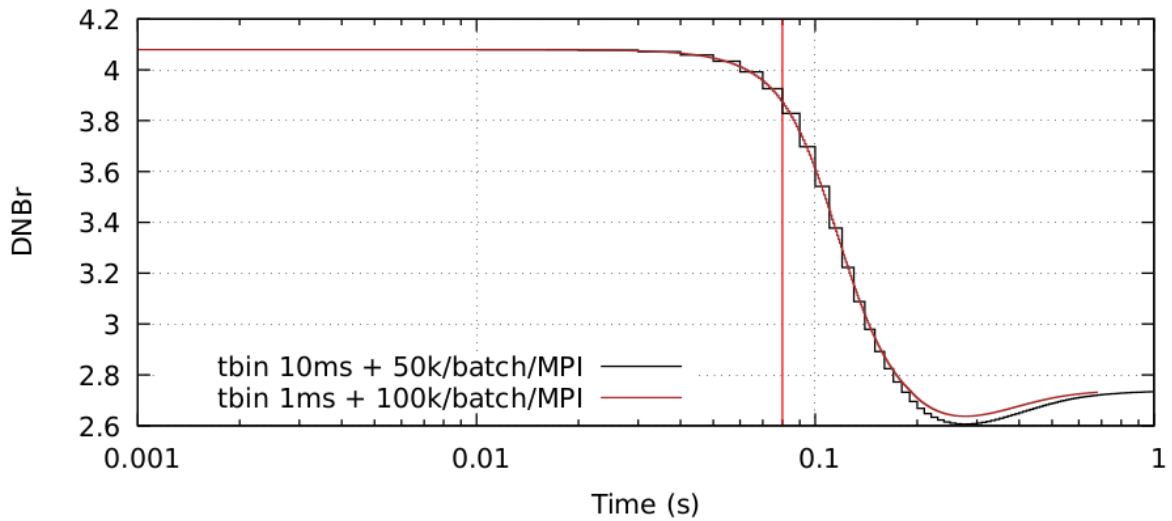


**FIGURE 32. MINIMUM DNB RATIO EVOLUTION IN TIME WITH W-3.**

A summary of the computation resources and simulation time are summarized in Table 18. Simulations are performed in the Horeka high-performance computing cluster [43]. Each CPU is an Intel Xeon Platinum 8368 with 76 cores per node.

**TABLE 18. COMPUTATIONAL RESOURCES AND SIMULATION TIMES.**

Case	MPI	OMP	Transient analyzed	Wall-clock simulation time
A	20	76	[0 – 2s] <sup>17</sup>	1 day
B	20	76	[0 – 1s]	20 hours
C	20	76	[0 – 0.682 s]	3 days

In conclusion, the analysis presented shows that time bin choices for SERPENT2 (time steps for SUBCHANFLOW) have a significant influence in fast transients (e.g. control rod ejection transients), especially in the power peak values, and the reason is mainly due to the rate in which fields between the codes are interchanged. In addition, shorter time bins in SERPENT2 lead to an increase in uncertainties, as observed in cases A and B. In case C, an increase in the number of primary particles was decided to have better statistics, but in combination with the shorter time bin of 1 *ms*, the computational resources increase very high, not allowing to finish the transient scenario due to wall-clock limitation times on the HPC configuration. Nevertheless, restart files can be considered in future to tackle these wall-clock issues<sup>18</sup>.

---

<sup>17</sup> Transient for case A was simulated up to 2 s but graphs only present up to 1 s.

<sup>18</sup> Acknowledgement: This work was performed on the Horeka supercomputer funded by the Ministry of Science, Research and the Arts of Baden-Württemberg and by the Federal Ministry of Education and Research.